CONSTRAINING CENOZOIC EXHUMATION
IN SOUTHEASTERN COLORADO AND EASTERN NEW MEXICO
USING LOW-TEMPERATURE THERMOCHRONOLOGY

Sabrina Josephine Hiu-Tung 簡曉彤 Kainz
Department of Geological Sciences
University of Colorado, Boulder (Territory of the Ute, Cheyenne, and Arapahoe people)

April 4th, 2022

Thesis Advisor:
Dr. Lon Abbott, Department of Geological Sciences

Defense Committee:
Dr. Rebecca Flowers, Department of Geological Sciences
Dr. Katherine Lininger, Department of Geography

ABSTRACT

The current elevation of the Southern Rocky Mountains and adjacent Great Plains are too high to be explained by crustal shortening during the Laramide Orogeny alone. Instead, we suggest that a later episode of epeirogeny affected the area. The mechanism behind this is ambiguous, but by constraining where and when potential Cenozoic uplift occurred, a more concrete history can be established. Surface uplift is often linked to exhumation via increased rates of erosion. This study focuses on finding spatial and temporal trends of exhumation in southeast Colorado and eastern New Mexico via low-temperature thermochronology, with the goal of linking regional thermal histories of multiple areas.

New apatite (U-Th)/He (AHe) data from the Spanish Peaks and surrounding basins in south-central Colorado present dates from 18-8 Ma, allowing us to infer kilometer-scale exhumation took place during the Miocene. Slightly older dates are found in the Chico Hills of northeast New Mexico at 22-13 Ma. At Two Buttes, 200km east of the Spanish Peaks in the Great Plains, an older Oligocene exhumation is observed (27.1 ∓ 4 Ma). To constrain the southern extent of this area, in central-eastern New Mexico, AHe and apatite fission track (AFT) data (Landman, 2016; Kelley & Chapin, 1995; Kelley & Duncan, 1986) were analyzed, showing a similar Oligo-Miocene, eastward oldening trend. Landman (2016) also found Oligocene AHe at Capitan Pluton in southern New Mexico.

Overall data patterns show mid-Miocene exhumation taking place in east-central New Mexico, with dates getting older to the west, east, and south. This pattern of erosion is best explained through regional epeirogeny with the focus of a more rapid and recent uplift being in east-central New Mexico. Only the Spanish Peaks region is inconsistent with this trend, with dates as young as 8 Ma being found. We hypothesize these youngest AHe dates are due to possible drainage reorganization of the Arkansas River that may have rerouted through the Great Plains of Colorado 5-10 m.y.a.

TABLE OF CONTENTS

1. Introduction

The Rocky Mountains and Great Plains of Colorado and New Mexico sit at unusually high elevations, unable to be explained by the magnitude of crustal shortening experienced during the last major mountain building event during the Late Cretaceous, the Laramide Orogeny (English & Johnstone, 2010). A typical mountain range formed by subduction is not expected to raise both mountains and adjacent plains to well over a mile high. With areas such as the Colorado Front Range sitting at a height above sea level of 1.6 km, the mystery of their origin is highly debated in the geology of the American West.

To solve the mechanism behind their existence, the time at which they reached their elevation must first be established. Current studies in central and northern Colorado have established post-Laramide dates of exhumation using low-temperature thermochronology (Abbott et al., 2022). My study focuses on the eastern extent of the Rocky Mountains in South-central Colorado, and into the Great Plains of Colorado and New Mexico, to determine trends and patterns of exhumation. I aim to investigate the timing and spatial extent of exhumation to provide a greater understanding of Post-Laramide Orogeny mechanisms of erosion occurring in the Southern Rocky Mountains and Great Plains. By targeting areas over 500 km north to south, and 400 km east to west, my goal is to constrain the similarities and differences in timing and rates of exhumation.

1.1 Objectives and Study Area

This study presents new Apatite Helium (AHe) data from three regions in Colorado and New Mexico. The work of Landman (2016) documented a south-to-north pattern of exhumation, using data from Capitan Pluton in southern New Mexico and the Spanish Peaks in southern Colorado. While presenting robust insight into the exhumation of the Great Plains, these targets were spaced over 400 km apart. My goal is to fill in the gaps by targeting three regions: (1) South-central Colorado, in the same area as Landman's (2016) Spanish Peaks data, but from lower elevation igneous bodies, (2) the Chico Hills in northeast New Mexico, and (3) Two Buttes, to gain information about the exhumation further out in the plains of southeast Colorado (Figure 1). All these targets have the advantage of containing igneous intrusions, suitable for low-temperature thermochronologic studies. Once surrounded by sedimentary rocks, these igneous intrusions record the timing at which erosion wore down these units.

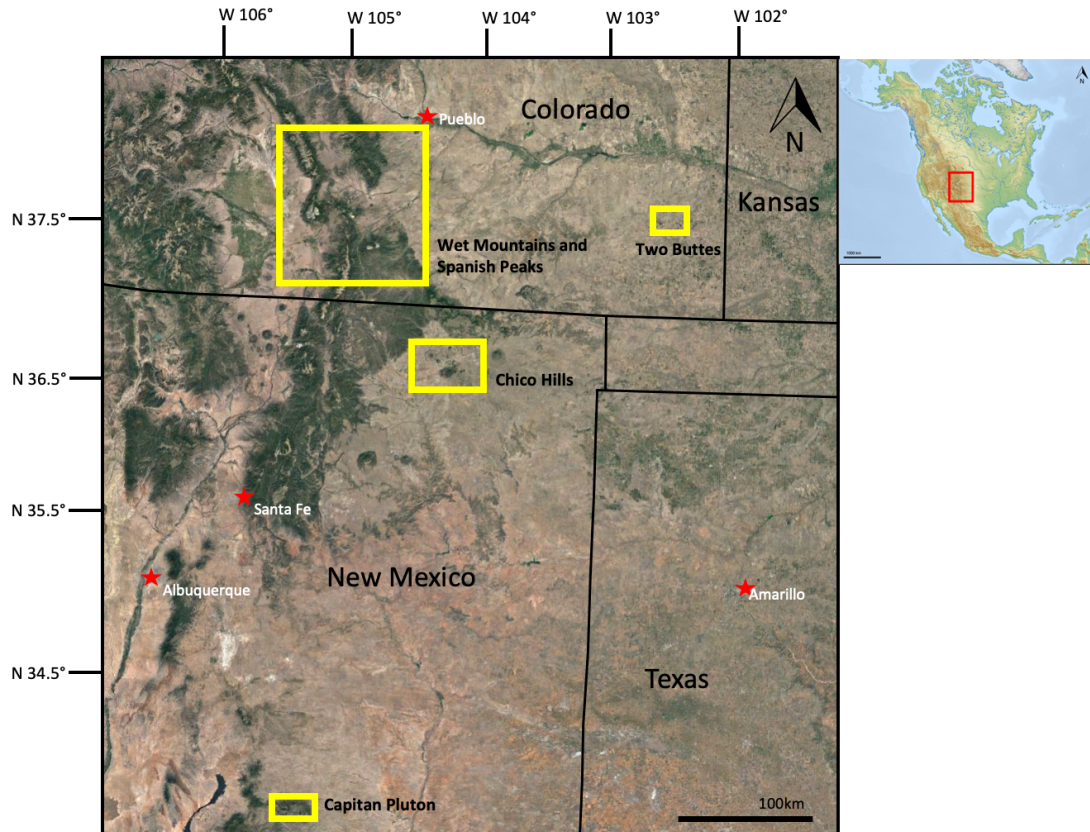Figure 1: Study regions. Areas with AHe low-temperature thermochronology are highlighted in yellow boxes.

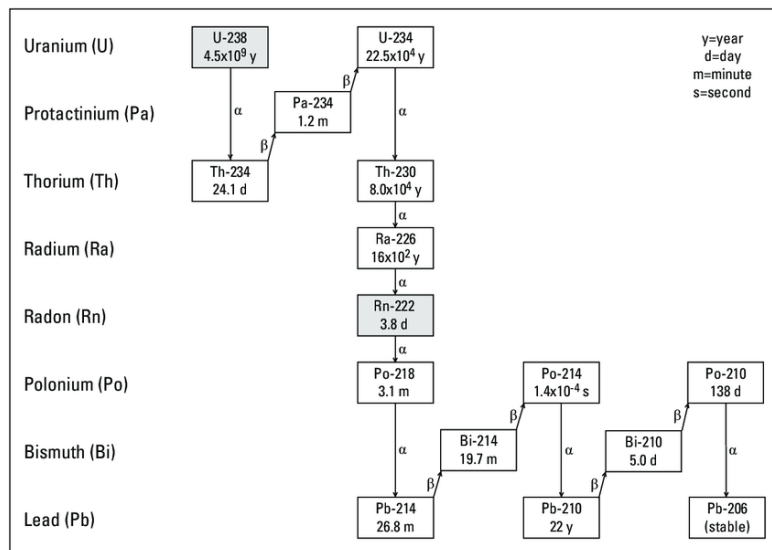## 1.2. Apatite (U-Th)/He Low-temperature Thermochronology

Figure 2: Example of ^{238}U decay chain, a major radiogenic parent nuclide used in low-temperature thermochronology. The other key measurement is of α-particles produced throughout the multi-phase decay (Ayotte et al., 2007).

Low-temperature thermochronology is a subset of geochronology in which radioactive decay products are used to determine the thermal history of a rock. (U-Th)/He thermochronology specifically looks at ^{238}U, ^{235}U, ^{232}Th, and ^{147}Sm as radioactive parent nuclides that release ^{4}He (α-particles) upon decay (Metcalf & Flowers, 2021). Minerals tend to have trace amounts of these radioactive elements, and have the ability to trap ^{4}He in their crystal lattice. However, when the mineral is too hot, it cannot retain the ^{4}He, and thus none can accumulate. Once the rock has cooled below a certain 'closure' temperature, it is capable of holding onto the ^{4}He. Low-temperature thermochronology studies the timing at which the rock has cooled enough to begin retaining helium.
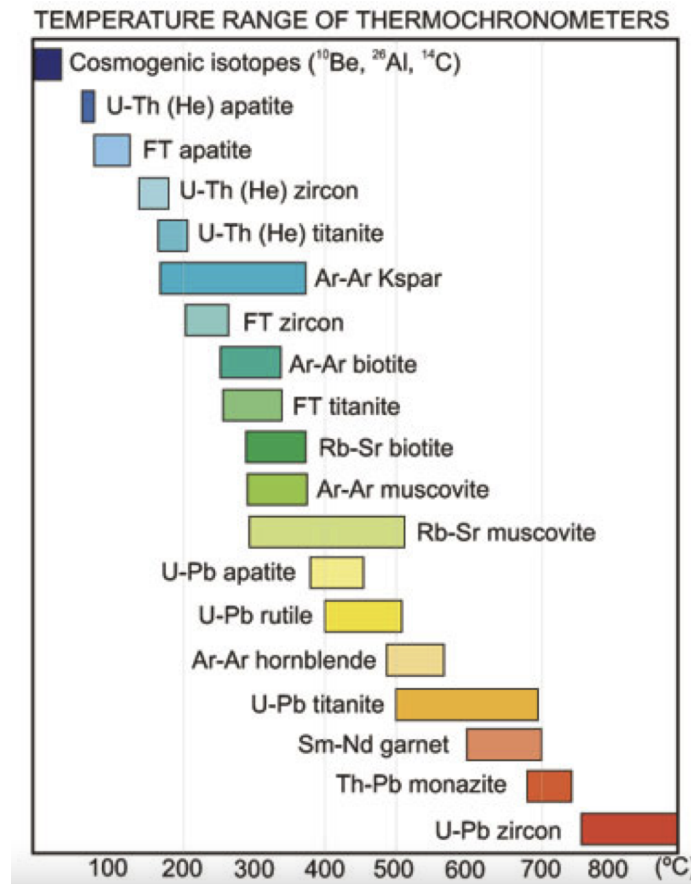
Figure 3: Closure temperature ranges of different minerals (Fitzgerald et al., 2002)

Apatite ($Ca_5(PO_4)_3(F,Cl,OH)$) has a closure temperature of ~70°C, making it one of the lowest temperature 'thermochronometers' currently established (Reiners, 2018). The depth at which this temperature is depends on the geothermal gradient of the crust but generally corresponds to around 1-3km depth below the surface (Metcalf & Flowers, 2021). Apatite (U-Th)/He is used in this study to investigate timing of exhumation. Previous studies cited in this work use apatite fission track (AFT) which has a closure temperature of ~110°C, correlating with depths of ~3.5 km. The use of multiple chronometers can help to establish rates of erosion.

2. Geologic Setting

The Colorado Rocky Mountains and Great Plains have a long and complex history of tectonic uplift, basin fill and exhumation. Pennsylvanian-Permian uplift during the Ancestral Rockies Orogeny formed the Ancestral Rocky Mountains that are theorized to have existed in Colorado. The change in base level promoted the erosion of many of these ranges, exposing crystalline rock throughout the region. The Wet Mountains, in what is now South-central Colorado, exemplifies basement rock of this age being brought to the surface. Synorogenic fill of basins adjacent to Ancestral Rocky Mountain ranges during the Late Paleozoic allowed for kilometer-thick sedimentary sequences to build up, including the prominent Sangre de Cristo Formation present throughout our study region (Figure 13).

During the Cretaceous, the transgression of the Western Interior Seaway covered Colorado and New Mexico in a shallow ocean. By this time, the topography of the Ancestral Rocky Mountains had been eroded down and evened out by Paleozoic sediments, allowing for further accumulation of shales and limestones (most notably the petroleum-bearing Pierre Shale). Despite being present for around 30 million years, differential coverage existed throughout Colorado. Isopach studies found that northern Colorado units were thicker than those found in the south (Cross & Pilger, 1978), which has the potential to bury and reset thermochronology dates to different extents.

Beginning in the Late Cretaceous, southern Colorado and northern New Mexico experienced a second mountain building event, the Laramide Orogeny, that would be responsible for bringing much of the Precambrian material that makes up today's Rocky Mountains to the surface. Shallow subduction of the Farallon Plate under the North American Plate resulted in compression that uplifted the Rockies further inland on the continent, rather than them being further West as expected for typical slab subduction (Jones et al., 2011).

Uplift, coupled with eustatic sea level drop, led to subsequent drainage of the Western Interior Seaway. One of these Laramide ranges includes the Sangre de Cristo Mountains, made from Paleozoic sedimentary sequences, from which we use Apatite Helium (AHe) and AFT dates described by Lindsey et al, (1986) and Ricketts et al, (2015). Faulting action during the Laramide also thrust the Precambrian material of the Wet Mountains over sedimentary material. The contrast of the sedimentary versus crystalline lithology of these two ranges that are in such close proximity to one another provides the setting to which we can study the effects of resistivity upon interpretations of low-temperature thermochronologic dates (Section 5.1)

The balance between uplift and denudation tipped towards the latter during the late Eocene when compression of plates stopped. Warm and wet climatic conditions led to the formation of the Rocky Mountain Erosion Surface (RMES) (Chapin & Kelley, 1997). The Wet Mountains and Sangre de Cristos were eroded, filling the Wet Mountain Valley, Raton Basin, and Denver Basin (Figure 13), till very little topography created by Laramide uplift remained.

Continuing into the Mid-Cenozoic Era, the ranges and Great Plains were soon covered by masses of volcanic ash during the Ignimbrite Flare-up from 37-24 Ma (Abbott & Cook, 2012). Other igneous bodies during this first volcanic episode relevant to this study are seen throughout the Rockies. An important feature we focus on is a lava flow atop Greenhorn Mountain at the southern extent of the Wet Mountains, dated at 33.4 ± 0.57 Ma by $^{40}Ar/^{39}Ar$ (McIntosh & Chapin, 2004) (Figure 8). This extrusive

body marks the surface at the time of its formation. Today, it lies at an elevation of ~3500m, over 1.5km above the modern surface of the adjacent plains a mere 15 km east. This dated surface is important for determining the timing of erosion in the Wet Mountains region.

At about 28 Ma, extension began in Colorado and New Mexico leading to the formation of the Rio Grande Rift Valley, responsible for another episode of intraplate magmatism. The Late Miocene (~7 Ma) brought about a series of SW-NE trending volcanic fields called the Jemez Lineament. This was the second episode of volcanism to take place in the Chico Hills complex of northeast New Mexico (Scott, Wilcox & Mehnert, 1990).

Thick conglomerate and sandstone sequences began building up in the Great Plains from runoff in the mountains, forming the Ogallala Formation. The base of the formation has been dated at 12-9.5 Ma, telling us when deposition began (Smith et al., 2016; Zakrzewski, 1988; Tedford et al., 2004).

Intraplate magmatism, from throughout Colorado's history, emplaced many shallow igneous intrusions targeted in this study (Figure 1): (1) the Spanish Peaks, two silicic to intermediate magma chambers emplaced at ~24 Ma (^{40}Ar/^{39}Ar dates from Penn & Lindsey (2009)) and (2) the hundreds of radial dikes originating from them, (3) Huerfano Butte, three vertical ultramafic dikes, northeast of the Spanish Peaks (25.2 ± 0.25 Ma from Penn & Lindsey (2009)), (4) the Chico Hills Sill Complex in Northeast New Mexico (36-24 Ma (Staatz (1985); Scott, Wilcox & Mehnert (1990)), (5) Two Buttes lamprophyres in the Great Plains of SE Colorado (36.8 ± 0.4 Ma K-Ar) (Davis et al. (1996)), and (6) Capitan Pluton in southern New Mexico (31 ± 4 Ma ZHe) (Landman, 2016).

The continued rise of the Colorado Rockies and Great Plains since the Laramide Orogeny has led to the elevations seen today, although the mechanism by which this occurred is still highly debated. This study intends to shed light on the rates and extent of exhumation to support any theories under consideration, with the goal of further understanding why the Rockies we see today are so high.

3. Methodology

3.1 Field Methods

Figure 4: (top left)Field sampling equipment next to an outcrop including a rock hammer, sledge, and gallon-sized bags, in the Chico Hills, NM (July, 2021); (top right) the Spanish peaks in south-central Colorado looking south; (bottom left) Eagle Rock Dike along the I-25 in the Chico Hills, NM; (bottom right) Two Buttes lamprophyres in southeast Colorado.

The first of two sample collection trips took place in July of 2020, with the intention of collecting igneous intrusions for a ~2km vertical transect in the Wet Mountains-Spanish Peaks region of

South-central Colorado. We targeted samples using the geologic map of the Trinidad Quadrangle (Johnson, 1969). With an intended 200m of elevation between these samples, we hiked to these locations and used a hammer and chisel to fill gallon-sized plastic bags.

The second trip occurred in July of 2021 and focused on collecting samples further south in the Chico Hills of New Mexico, as well as at Two Buttes Dam and Wildlife Area, Baca County, Colorado. Here, less relief meant a vertical elevation transect could not be sampled, but rather the lateral footprint was studied to determine the spatial extent of any detected exhumation.

Sampling of weathered rocks on the surfaces of outcrops were avoided in the field in favor of fresh exposures underneath. Exact locations were marked with GPS waypoints that would later be placed on Google Earth.

3.2 Mineral Separation

A total of 16 samples were processed for this study with the intention of finding Apatite Helium (AHe) dates: 2 collected by Lon Abbott in 2019/2020, 8 collected from South-central Colorado in 2020, and 6 from NE New Mexico and Two Buttes in 2021.

Dating of apatites was chosen due to their resistance to break down and their ability to retain ^{4}He. This is used, in the context of this study, to link the timing at which an igneous body was close enough to the surface to cool below ~70°C. Geothermal gradients throughout Colorado's history dictate that apatites cool to ~70°C at around a 1-3 km depth below Earth's surface (Metcalf & Flowers, 2021). The 2 km depth range is due to uncertainty in the actual geothermal gradient at the time of exhumation.

Figure 5: Mineral separation techniques including crusher/grinder (left), water table (center), and magnetic separator (right).

As apatites are the target grains, a series of steps to isolate these grains are run using the equipment available in the University of Colorado Boulder's SamPLER Laboratory and the Thermochronology Research and Instrumentation Laboratory (CU TRaIL Website). The procedure for isolating apatite minerals is described below.

Rocks from the field are first run through the BICO rock crusher and disk mill. A hand sample around 8-10cm wide was kept from each gallon bag so macroscopic observations could be made when the rest of the sample had been crushed. The crushing/grinding process allows the majority of the sample to be ground down to a desired <500μm, which is separated from larger grains using 500 μm mesh sieve openings.

The <500 μm sample is put through a Wilfley table for water separation. Four containers are placed below the table (W1-W4) that collect the grains once they are washed off. Grains are propagated by the influences of gravity through the shaking water table, wherein denser grains are carried further

along to the bottom left of the table and fall off into the W1 container. Lightest grains are washed down quicker into W4. As much of the sample is dust, the water washes it away so the sample is clean for subsequent steps. All containers are dried in an oven for 24-48 hours at 65°C. Apatite grains are found in greatest concentrations in W1, so W2-W4 are stored away. In the case that W1 has a low apatite yield, W2 is processed in the next stage of magnetic separation.

A Frantz magnetic separator is used to remove magnetic grains from desired non-magnetic apatites. Particularly heavy and darker samples are usually indicative of high concentrations of magnetic grains (e.g. magnetite), and thus a hand magnet is used before running the sample through the Frantz. This is intended to reduce blockages in the machine and remove the most magnetic material. The W1 sample is loaded into a vibrating cylinder that slowly feeds grains onto a metal tray positioned at a 20° angle. An electromagnetic field keeps more magnetic grains in a straight line while non-magnetics fall to the bottom of the tray. These two streams are then collected in separate containers. The current can be changed so as to control the intensity of the generated electromagnet. The sample is first run through 0.35A, then the non-magnetic separates are again run using 0.6A. Two phases of this separation take place to avoid clogging the Frantz by attempting to remove all magnetics at once.

Non-magnetic grains that are not removed by 0.35A or 0.6A are moved to the stage of heavy liquid separation. While the majority of other rock-forming minerals are magnetic enough to be removed in the previous step, quartz, feldspar and a few other minerals remain in the non-magnetic separates. Thus, to isolate apatite, heavy liquid separation is needed. The sample is split between 8 plastic vials (50 ml each) depending on the amount of non-magnetic yield. 7.5ml of sample is put in each vial, which is then filled to the 45ml mark with Lithium Metatungstate (LMT) (ρ=2.85-2.90 g/cm^3). Apatite has a density of 3.16-3.22 g/cm^3 where many common minerals are less dense(e.g. quartz, plagioclase, etc.) meaning the targeted apatites will naturally sink and undesired grains will float to the top of the vial. To aid this process, vials are run through a centrifuge for 2 minutes at 2000 rpm. Vials are balanced in the centrifuge by running either 2, 4 or 8 at a time to maintain symmetry. Removing the less dense material requires the use of liquid Nitrogen capable of freezing LMT. The bottom third of each vial is submerged in the Nitrogen for 1.5 minutes to lock the heavy material in place before a pick is used to pour the liquid LMT and lighter grains out. Vials with frozen LMT are allowed to thaw before coalescing the heavies together to be inspected under a petrographic microscope.
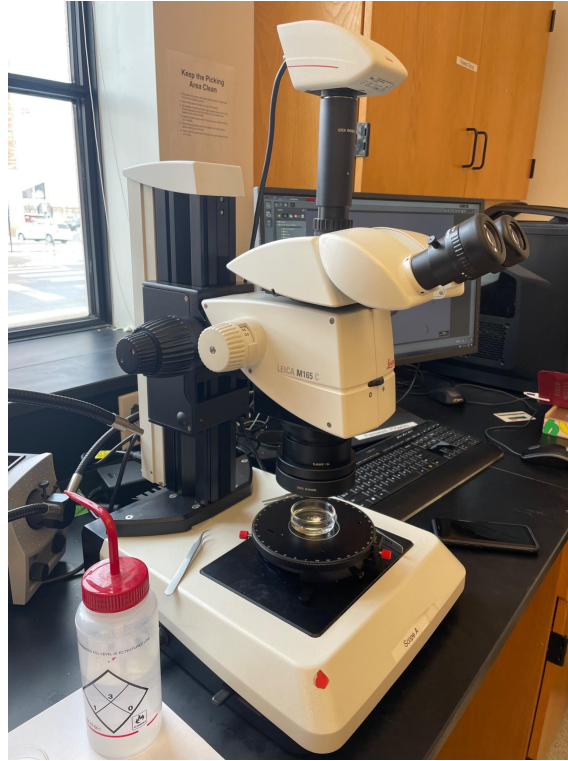
3.3 Apatite selection and preparation

Figure 6: Leica M165 C petrographic microscope used for picking apatite grains

A petrographic microscope is used for grain selection. The (U-Th)/He system uses single-grain aliquots, so selecting the appropriate grains to run is essential to reliability in data. Apatite crystals are picked with tweezers from the LMT heavies emptied into a petri dish, which are submerged in ethanol to lessen refractive index contrast (Reiners et al., 2018) and reduce movement of grains within the dish. Crystals are identified by their hexagonal shape that terminate in two blunt caps on either end of the C-axis. However, grains are most commonly broken perpendicular to the C-axis, meaning they often lack one or both terminations. Under plane polarized light, apatites are clear and pleochroic. Under cross polars, they exhibit low birefringence, usually as 1st order gray to yellow that vary with thicknesses. Selection of grains considers: (1) morphology, (2) grain size and thickness, and (3) presence of inclusions. (1) Generally, euhedral grains are preferred as rounding adds uncertainty to He-loss. Loss of terminations, cracks and chipped faces are not ideal, though can still be run if no other grains are found. (2) Grains less than 80 μm wide are discarded as they are not able to retain enough ^{4}He. The process of alpha-ejection propels ^{4}He ~15-20 μm from the location of decay (Metcalf & Flowers, 2021), so grains that are too small have too much uncertainty to produce reliable results (Figure 7). (3) Finally, both mineral and fluid inclusions are to be avoided. Such inclusions may contain U and Th, which affects results of how much parent to daughter nuclide is recorded. A typical sample is picked until five suitable grains are found. Minerals are then placed in niobium packages using forceps to cinch a metal tube on both sides.
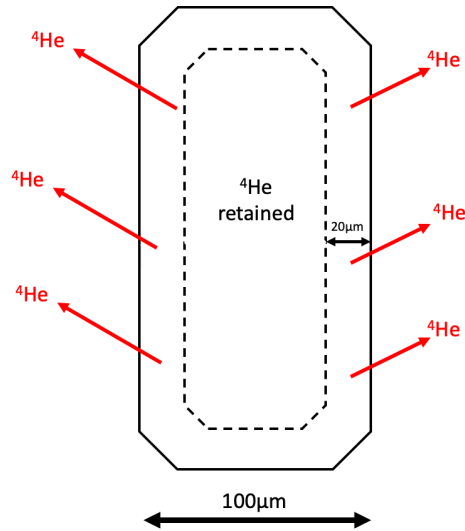
Figure 7: Apatite grain showing alpha-ejection zone, at which ^{4}He is diffused regardless of is the grain has cooled below its closure temperature. The measured ^{4}He is that which accumulates within the dashed volume.

3.4 (U-Th)/He Analysis

Measurement of accumulated daughter (^{4}He) and parents (U-Th-Sm) nuclides was done in the CU TRaIL lab by Dr James Metcalf and Dr Jeffery Benowitz.

First, packed apatites are run through the Australian Scientific Instruments (ASI) Alphachron for degassing and measurement of ^{4}He. Niobium tubes are placed in an ultrahigh vacuum chamber (UHV) and subjected to heating via diode lasers (900-1300 °C) (Reiners et al., 2018). Samples are then spiked with ^{3}He before isotopes are purged and measured with a Pfeiffer Balzers Quadrupole Mass Spectrometer (QMS) (CU TRaIL Website). Degassed grains are dissolved in nitric acid solutions. The Agilent 7900 Quadrupole Inductively Coupled Plasma Mass Spectrometer (ICPMS) measures the amount of parent isotopes used to reconstruct a date.

Alpha-ejection requires correction to estimate the amount of helium lost. Smaller grains eject a greater percentage of ^{4}He, which means there is more uncertainty in calculated dates (Metcalf & Flowers, 2021). To consider the reliability of a grain, an alpha-ejection factor (Ft) is calculated (Farley, 2002). Grains with an Ft < 0.65 are considered too small and the correction becomes too large to be accurate.

Effective uranium concentration (eU) is a calculated value that considers the relative decay of parent nuclides (U-238, U-235, and Th-232) to produce α-particles (Metcalf & Flowers, 2021). The eU of a grain is indicative of the amount of radiation damage experienced. The more the damage, the greater the eU due to altered He kinetics, which in turn means a higher closure temperature in the grain (Flower et al., 2009). In a sample of 4-5 apatite grains, the spread of interpreted AHe dates with varying eU gives information about the rates of cooling within the sample. The more positive the date-eU slope is, the slower the rock cooled. If it cooled quickly, it would pass through the range of closure temperatures in less time, and thus all eUs would be closer together in age (horizontal line on date-eU plot). We can use these correlations to make inferences about relative rates of cooling.

4. Results

27 AHe dates were found from 6 different samples. Each samples contains 4 or 5 apatite aliquots. Apatite helium (AHe) dates reported in the Discussion section are found in the Corrected Date (Ma) column. These consider the size of each apatite, and correct for alpha-ejection. Averaged dates for each sample use 1 standard deviation for uncertainties. LA20-1, SK21-1, and SK21-2 also have average dates with certain grains omitted. These take out anomalous data points, explained by low alpha-ejection factors (Ft).

Table 1: Single Grain Apatite (U-Th)/He Data

Sample	Aliquot[a]	Rs (μm)[b]	⁴He (nmol/g)[c]	±[d]	U (ppm)[c]	±[d]	Th (ppm)[c]	±[d]	Sm (ppm)[c]	±[d]	eU[e]	±[f]	Uncorr Date (Ma)[g]	Uncorr Date Analytic Unc. (Ma) 2σ[h]	F_T comb[i]	Corrected Date (Ma)[j]	Corr Date Analytic Unc. (Ma)2σ[k]
South-central Colorado																	
LA20-1: Huerfano Butte ultramafic lamprophyres, 37°45'13'' N, 104°49'38'' W, 1823m																	
	a01	60.8	0.34	0.00	3.6	0.1	31.6	0.5	116.3	1.8	11.3	1.7	5.64	0.09	0.746	7.53	0.24
	a02	48.7	0.55	0.01	4.1	0.3	32.2	0.6	147.9	2.8	11.9	1.8	8.60	0.23	0.686	12.47	0.64
	a03	75.7	0.62	0.01	6.1	0.2	51.3	0.4	115.7	1.1	18.4	2.8	6.25	0.10	0.795	7.85	0.24
	a04	53.3	0.25	0.01	2.8	0.0	18.2	0.4	130.4	2.5	7.3	1.1	6.26	0.18	0.714	8.72	0.49
	a05	51.7	0.19	0.00	2.8	0.2	17.5	0.2	135.8	1.5	7.2	1.1	4.98	0.15	0.705	7.01	0.43
															Avg + SD	8.71	2.19
															Avg +SD w/o a02	7.8	0.7
SK20-1: Porphyritic intemediate dike from the Spanish Peaks, 37°27'31'' N, 105°01'55'' W, 2272m																	
	a01	41.9	2.71	0.02	23.2	0.4	109.0	1.2	194.8	2.4	49.3	7.4	10.20	0.12	0.643	15.82	0.38
	a02	52.0	2.26	0.02	21.4	0.4	110.6	1.2	146.0	2.6	47.9	7.2	8.78	0.11	0.709	12.36	0.30
	a03	66.1	2.43	0.02	20.4	0.4	95.9	1.1	103.7	0.9	43.3	6.5	10.39	0.14	0.770	13.48	0.35
	a04	47.5	2.10	0.01	20.5	0.9	95.3	1.7	109.2	4.4	43.2	6.5	9.00	0.21	0.683	13.15	0.59
	a05	51.7	1.99	0.02	15.1	0.4	73.0	0.9	93.8	2.6	32.5	4.9	11.37	0.20	0.708	16.04	0.54
															Ave+SD	14.2	1.7
Chico Hills, NM																	
SK21-1: mafic Eagle Rock Dike, 36°39'55'' N, 104°29'42'' W, 1822m																	
	a01	38	1.3	0.0	7.3	0.8	49.1	1.3	197.2	5.2	19.2	2.9	12.4	0.6	0.61	20.3	1.8
	a02	44	1.0	0.0	9.4	0.2	49.6	1.2	155.4	2.9	21.4	3.2	8.9	0.2	0.66	13.4	0.6
	a03	41	2.5	0.0	13.2	0.6	83.2	1.3	238.2	6.1	33.3	5.0	14.1	0.3	0.63	22.3	0.9
	a04	33	5.0	0.0	25.7	1.6	174.6	3.9	415.0	10.9	67.8	10.2	13.6	0.4	0.55	24.8	1.2
	a05	39	0.7	0.0	4.0	0.4	25.4	1.1	157.5	6.0	10.3	1.5	11.9	0.6	0.62	19.2	2.0
															Avg + SD	20.0	4.2
															Avg + SD w/o a02&a04	20.6	1.6
SK21-3: Piney Mtn Rd tephrite, 36°32'52'' N, 104°09'20'' W, 2300m																	
	a01	63	5.0	0.0	6.8	0.2	256.4	4.4	140.2	2.0	68.0	10.2	13.5	0.2	0.75	18.1	0.6
	a02	58	10.0	0.1	13.1	0.2	480.8	7.5	204.6	3.3	127.8	19.2	14.5	0.2	0.73	19.9	0.6
	a03	42	19.2	0.1	56.9	1.4	1044.8	18.4	441.5	5.4	306.1	45.9	11.6	0.2	0.63	18.6	0.6
	a04	37	10.3	0.1	13.7	0.9	543.7	9.6	232.1	6.3	143.4	21.5	13.3	0.3	0.57	23.2	0.8
															Avg + SD	19.9	2.3
															Avg + SD w/o a04	18.9	0.9
SK21-2: Slagle trachyte, 36°37'21'' N, 104°15'58'' W, 2054m																	
	a01	58	3.1	0.0	13.8	0.3	138.6	2.3	227.4	3.1	47.1	7.1	12.3	0.2	0.73	16.8	0.5
	a02	75	5.0	0.0	20.8	0.3	293.0	4.6	146.1	1.9	90.7	13.6	10.2	0.1	0.79	12.9	0.4
	a03	43	3.7	0.0	17.5	0.4	170.0	2.9	315.7	5.1	58.3	8.8	11.7	0.2	0.65	17.9	0.6
	a04	72	3.0	0.0	17.5	0.4	134.6	4.0	129.2	1.1	49.6	7.4	11.2	0.2	0.78	14.3	0.6
															Avg + SD	15.5	2.3
Great Plains, SE Colorado																	
SK21-6: Two Buttes lamprophyres, 37°39'23'' N, 102°32'17'' W, 1326m																	
	a01	49	13.8	0.1	87.8	2.0	228.7	2.4	175.2	3.6	142.5	21.4	18.0	0.3	0.70	25.7	0.8
	a02	51	5.6	0.0	21.5	1.2	130.9	1.3	234.9	4.0	52.9	7.9	19.7	0.4	0.70	27.9	1.2
	a03	43	9.3	0.1	40.2	0.6	172.3	1.4	337.3	8.7	81.6	12.2	21.2	0.3	0.65	32.4	0.7
	a04	92	7.0	0.0	23.7	0.6	191.6	2.2	127.3	1.2	69.5	10.4	18.7	0.2	0.83	22.5	0.6
															Avg + SD	27.1	4.16

Shards of Durango Fluorapatite run in conjunction with these grains yield a date of 30.7 ± 1.5 Ma (2s SE, n=15)

a - Sample and mineral being analyzed. a is apatite, z is zircon.
b - Rs is the radius of a sphere with an equivalent alpha ejection correction as the grain, calculated using equation A6 in Cooperdock et al., (2019)
c - Concentrations of He, U, Th and Sm computed from their absolute amounts and the estimated dimensional mass reported in Table 3
d - 2s propagated analytical uncertainty on the U, Th, Sm, and He measurements
e - eU is effective uranium concentration. Calculated as U + 0.238*Th + 0.0012*Sm after Cooperdock et al., (2019)
f - Uncertainty on eU estimated at 15% of the eU value
g - Uncorrected date is calculated iteratively using the 4He production equation defined as equation 1 in Wolf et al. (1998) and assuming secular equilibrium.
h - 2s propagated analytical uncertainty on the U, Th, Sm and He measurements
i - The combined alpha-ejection correction for the crystal calculated from the isotope specific FT corrections in Table 2, the proportion of U and Th contributing to 4He production, and assuming homogeneous parent isotope distributions.
j - The corrected date is calculated iteratively using the absolute values of He, U, Th and Sm in Table 2, the isotope specific FT corrections in Table 2, and equation 34 in Ketcham at al., (2011) assuming secular equilibrium.
k - 2s propagated analytical uncertainty on the U, Th, Sm, and He measurements

5. Discussion

Discussion of data will be split up into two separate sections. The first section (5.1) details the lithologic effects on low-temperature thermochronology, using South-central Colorado's Wet Mountains and surrounding basins as a case study. The second section (5.2) focuses on larger scale patterns of exhumation in southeast Colorado and eastern New Mexico, followed by possible causes of these trends. Finally, section 5.3 details errors and uncertainties within this study.

5.1. Effects of rock erodibility on thermochronology data and exhumation interpretations

Flowers & Ehlers (2018) highlight the importance of considering differences in rock erodibility when interpreting low-temperature thermochronology data. Most ranges in the Southern Rocky Mountains are composed of Precambrian basement with low erosion potential due to their strong crystalline material. Flowers and Ehlers (2018) point to this as the cause for Laramide AHe and AFT dates (55-70 Ma) as opposed to younger dates that would be triggered by post-Laramide exhumation, such as those we have documented in South-central Colorado.

The difference in low-temperature thermochronometric dates for the Wet Mountains compared with surrounding areas provides an excellent opportunity to study how lateral variations in rock erodibility can cause dramatic differences in topography and exhumation rates, providing an example of how interpretations these dates should consider this as a factor as suggested in Flowers & Ehlers (2018). The variability of AHe and AFT dates from a number of studies in the region, including this study, are attributed in part to the rock types present.
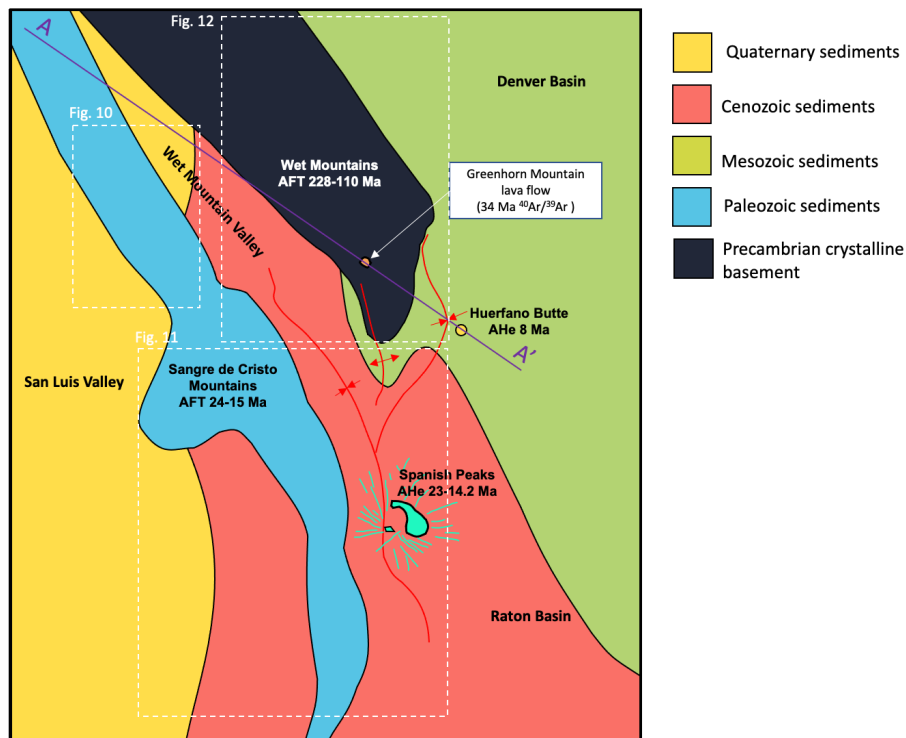

Figure 8: Simplified geologic map of South-central Colorado; Line A-A' represents the cross section seen in Figure 13.

The Wet Mountains form a peninsula of Precambrian basement that juts into the sedimentary foreland basins that surround it to the east, west, and south (Figure 8). The areas dominated by sedimentary material record our proposed Miocene exhumation event. Although these softer rocks are rarely targeted for sampling, igneous intrusions (e.g. Huerfano Butte and East Spanish Peak) exposed on the surface record timing of erosion of sedimentary material that once surrounded them. These are great targets not just because they are igneous (i.e. won't have detrital dates), but also because they tend to be more resistant to erosion and stick out in the landscape as a result. In addition, sedimentary rocks that have been buried deep enough by pre-existing sequences also provide low-temperature thermochronology. For example, the Paleozoic sediments of the Sangre de Cristo Mountains were thrust into stacked sheets during the Laramide, burying the now-exposed sedimentary rocks deeply enough to reset AFT dates. We can take this concept of differential rock strengths to the regional scale to understand why thermochronology dates are so varied throughout the Wet Mountains compared to adjacent basins.
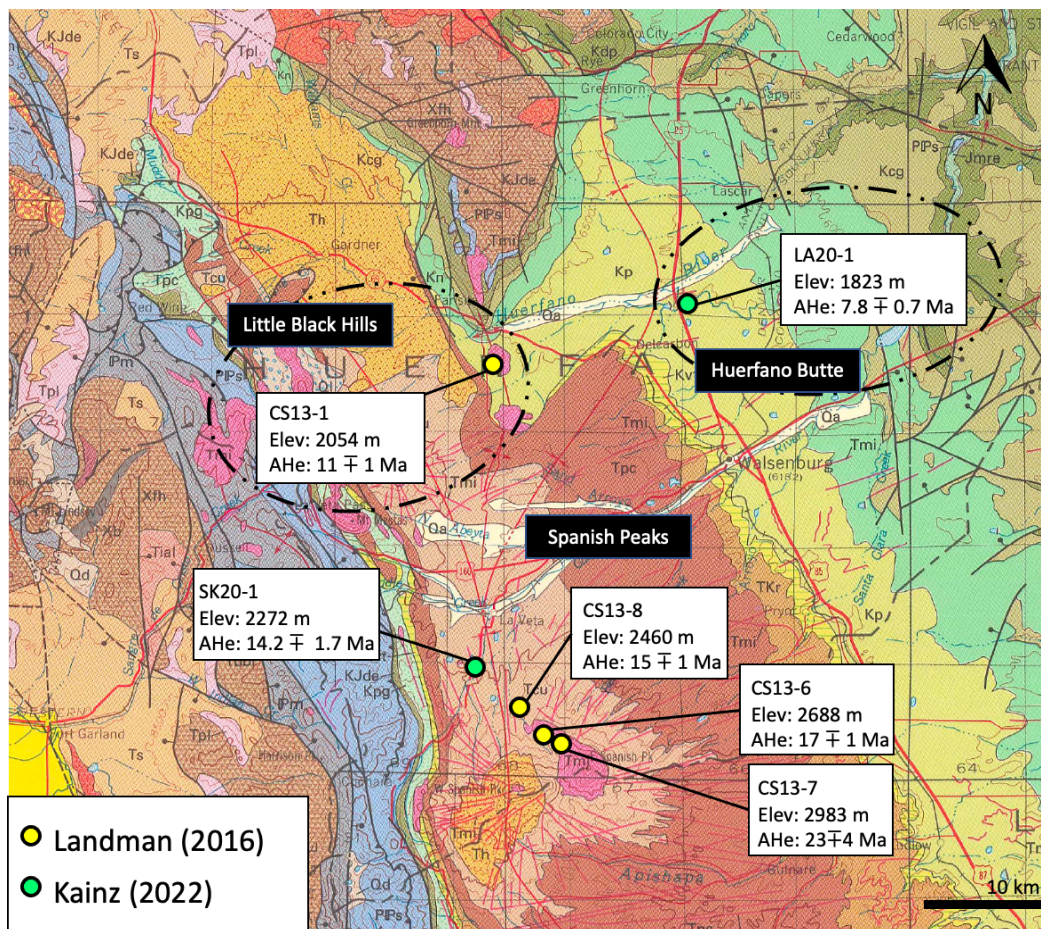

Figure 9: AHe dates from the Raton Basin. These include data from the Spanish Peaks, the Little Black Hills, and Huerfano Butte.
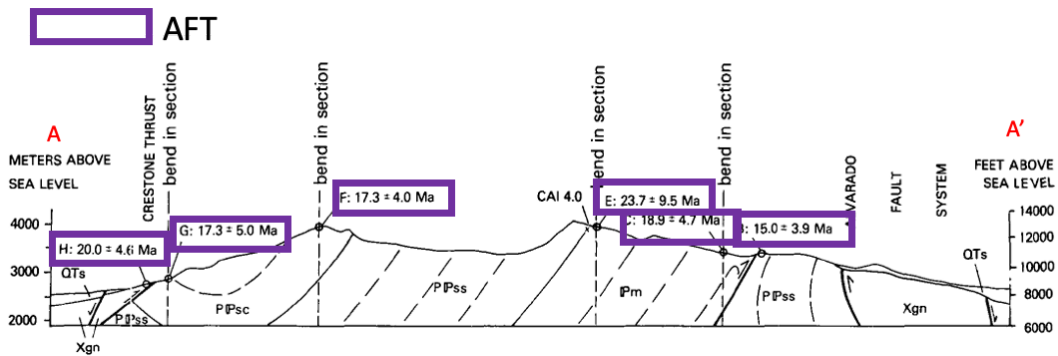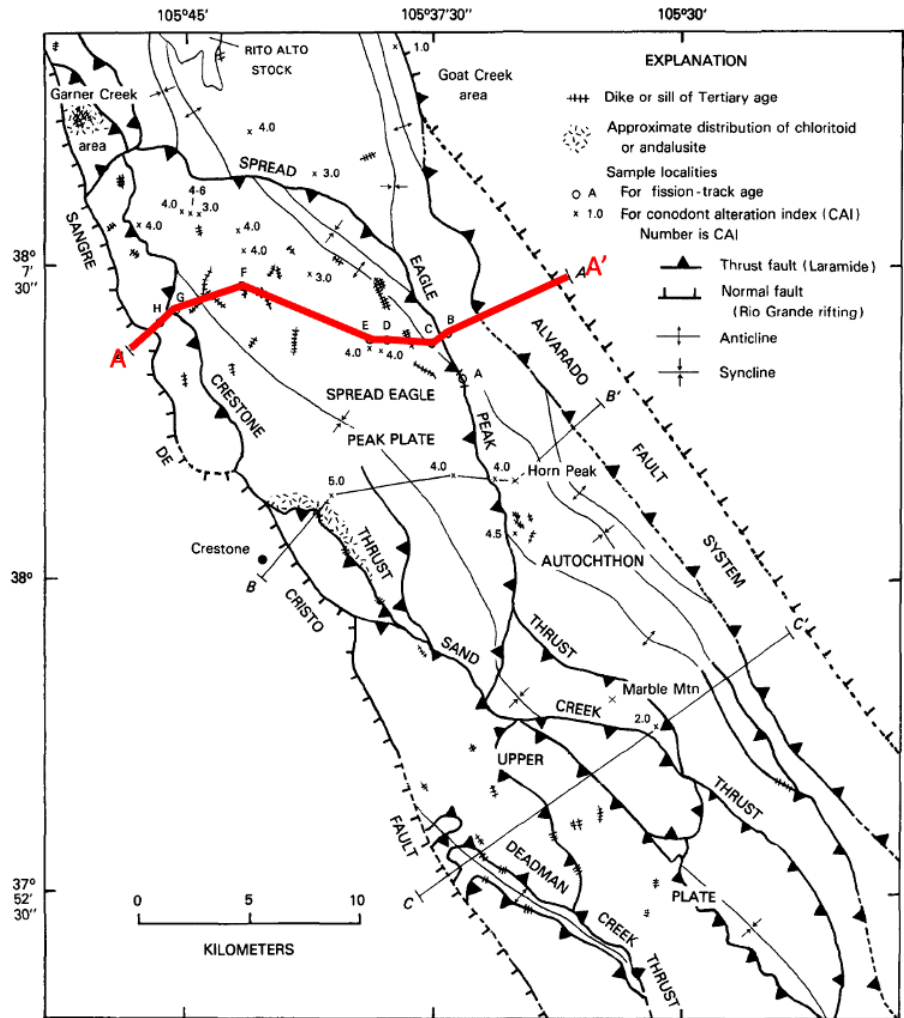
16

Figure 10: AFT data from the Sangre de Cristo Mountains in South-central Colorado (Lindsey et al., 1986) showing a cross section (A-A') of post-Laramide dates.
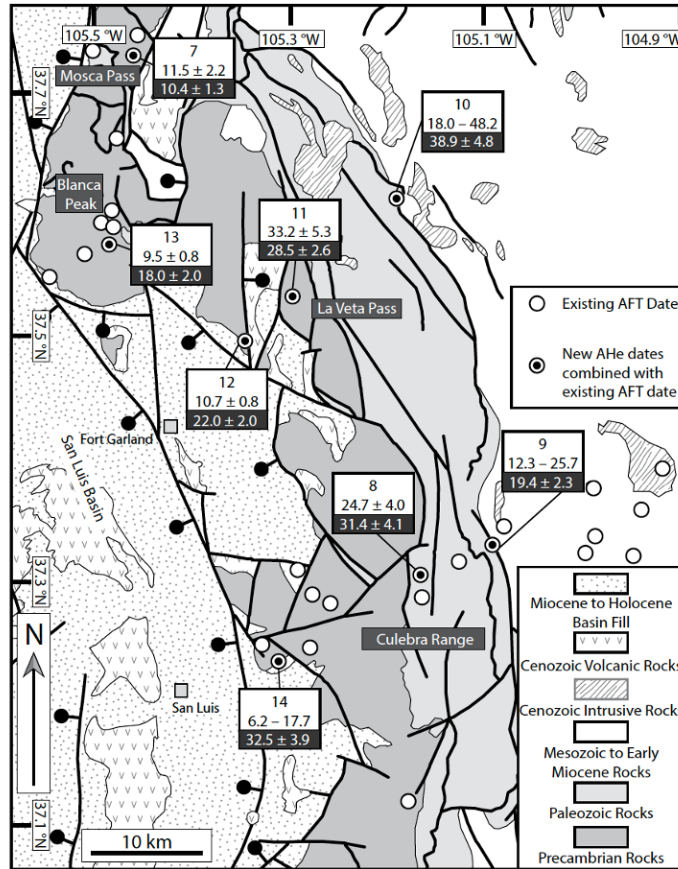
17

Figure 11: AHe dates from Ricketts et al. (2015) added to the Sangre de Cristo Range atop of existing AFT dates from Kelley et al. (1992).

Looking first to the Spanish Peaks, these igneous bodies were intruded into what is now the Raton Basin, composed of synorogenic fill from erosion during the Laramide Orogeny and Cretaceous marine deposits. The post-Laramide erosion of the basin, triggered by our explored exhumation, records nearly 2 km of vertical erosion since the Miocene using AHe (Landman, 2016) (Figure 9). Similar AFT dates at 24-15 Ma are also found 30km northwest in the Sangre de Cristo Mountains (Lindsey et al., 1986). AFT measures the time at which the samples were shallower than ~3.5km below the surface suggesting an even larger magnitude of exhumation was taking place, consistent with the AHe dates in the Raton Basin. Ricketts et al. (2015) then completed AHe work further south, in the Culebra Range of the Sangre de Cristos, showing some parts of the mountains eroding through to 10 Ma (Figure 11). Our study expands this pattern to the east of the Wet Mountains at Huerfano Butte, showing exhumation till 8 Ma in the Raton Basin at an elevation of ~1800m.
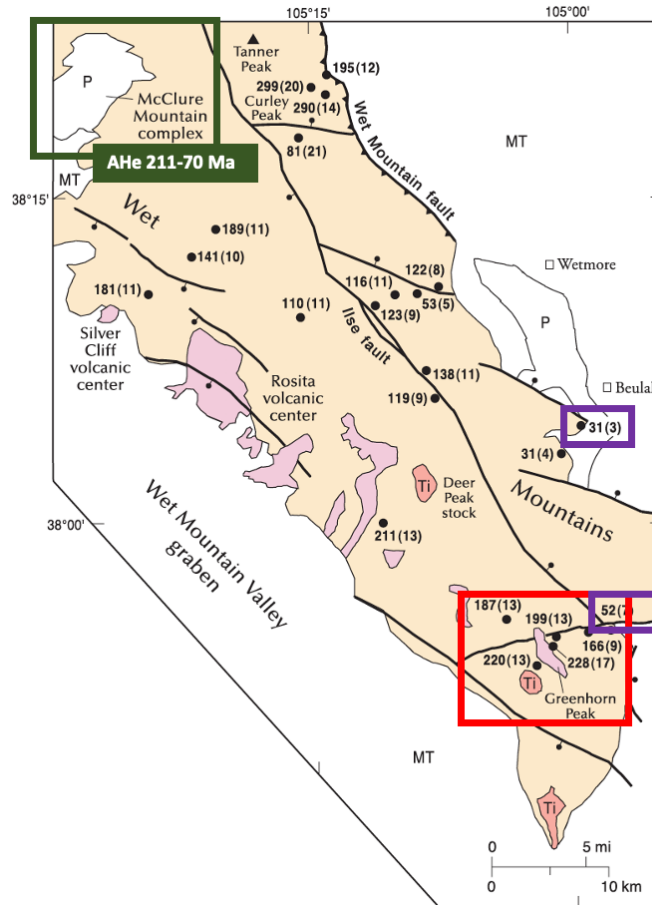
Figure 12: Wet Mountains AFT dates from Kelley & Chapin (2004). Dates are in millions of years with standard age error in brackets. Green box and dates are AHe from the McClure Mountain Syenite (Weisberg et al., 2018). Red box added represents samples that were likely on the RMES as they are at the highest elevations and are closest to the Greenhorn Peak ash flow tuff (paleosurface). Purple boxes show the youngest AFT dates. Note that these are still older than Miocene AHe dates from this study, and that they reside on the lowest elevations at the edge of the Wet Mountains.

If we now focus on the Wet Mountains, AFT and AHe data shows a much older range of dates, going as far back as the Early Permian (Kelley & Chapin, 2004; Weisberg et al., 2018) (Figure 12). The pre-Laramide dates likely stem from the former presence of <3.5km of sediment cover overlying the basement, and thus AFT dates were not reset when that cover was subsequently eroded. Although the youngest values from this dataset record Eocene exhumation (52-31 Ma), this still precedes the Miocene dates in the basins and Sangres to the east, south, and west. These younger dates (Figure 12) also are from samples at the low elevation edges of the Southern Wet Mountains, which Kelley & Chapin (2004) suggest represent heating to 95-110°C from volcanism in the Oligocene, coinciding with emplacement of features such as the Spanish Peaks.

Another geological feature that gives indisputable evidence about the Wet Mountains' history is the Greenhorn Mountain lava flow (Figure 8). Sitting at the top of the high elevation Southern Wet Mountains, this lava flow must have once been at a topographic low along the RMES. Dated to be 34 Ma (Mcintosh & Chapin, 2004), the Wet Mountains would not have had the relief seen today during its emplacement. So, the fact that it now lies nearly 2km above the adjacent basins means the Wet Mountains must have experienced minimal erosion compared to sedimentary sequences.

With AFT and AHe data to the east, south, and west of the Wet Mountains all agreeing on exhumation during a post-Laramide event, the question as to why the mountains in between have significantly older dates is posed. How is it possible that such a stark contrast in thermochronologic dates is found over relatively short distances laterally? The obvious difference between these localities is their lithology and associated resistances of material. The Wet Mountains are composed of crystalline basement rock that is relatively difficult to erode. On the other hand, the Sangre de Cristos are made of softer Paleozoic sedimentary sequences, and basins to the south and east are even less consolidated with sediment that is not as strongly lithified. Crystalline rock erodes at much slower rates, leading to negligible amounts of material lost post-Laramide in the Wet Mountains. In contrast, sedimentary rock is much more susceptible to break down and thus will lose much more height over the same period of time (Flowers & Ehlers, 2018).
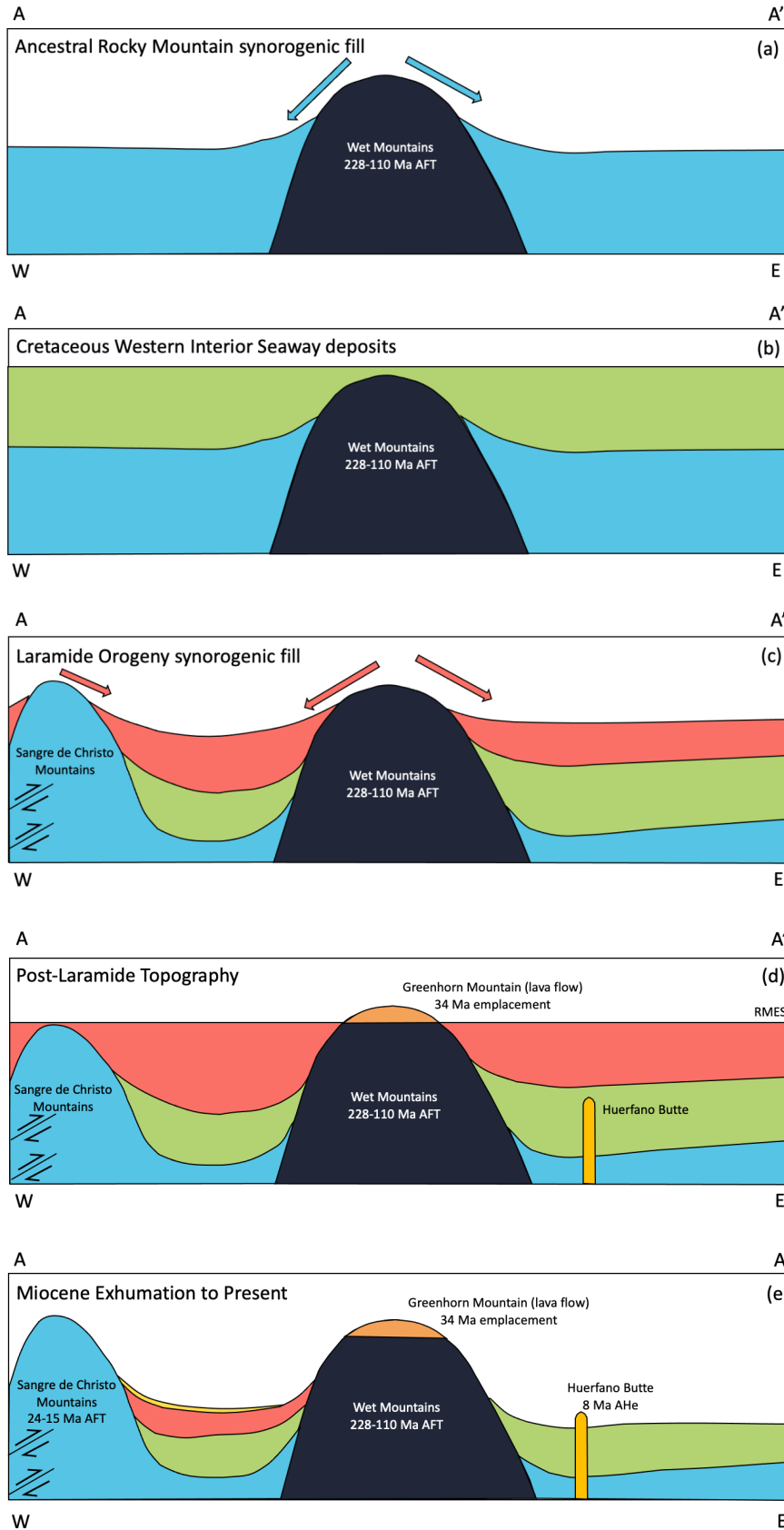
Figure 13: Cartoon cross section A-A' from Figure 8 showing differential erosion since the Late Carboniferous. (a) Rise of the Ancestral Rocky Mountains expose the crystalline rock (black)of the Wet Mountains and Paleozoic synorogenic fill adjacent (blue). (b) The Western Interior Seaway covers the region with marine to coastal deposits such as the Pierre Shale (green). Burial of the Wet Mountains is likely < 3.5 km thick as AFT dates are not reset. (c) Uplift in the Laramide forms the Sangre de Cristo (SDC) Range from Paleozoic sediments, and the Wet Mountains. Compression thickens the SDC by creating thrust faults. Synorogenic fill from both ranges deposits Cenozoic sediments (salmon) in basins. (d) Laramide topography is evened out to the Rocky Mountain Erosion Surface (RMES). Sediment in the basins rises to similar levels as lowering ranges. The Greenhorn Mountain ash flow tuff is emplaced on the surface at a topographic low, and Huerfano Butte is intruded at > 1.5-2 km depth. (e) Exhumation in the Miocene erodes sedimentary basins much faster, leaving the Wet Mountains ~2km above them. All Cenozoic sediment in the Raton Basin to the east is eroded, exposing Huerfano Butte in Mesozoic material. Isostatic rebound helps raise the Wet Mountains. Thin Quaternary deposits exist in the Wet Mountain Valley.

21
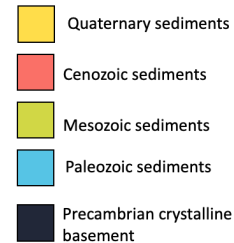
The basement rock that makes up the Wet Mountains was first uplifted during the formation of the Ancestral Rocky Mountains as discussed in the Geologic Settings. It is possible that rapid erosion of sedimentary rock previously overlying it was quickly shed off and deposited in adjacent valleys. Once the bedrock was exposed, much slower rates of erosion began, leading to the AFT dates recorded from this period. The onset of the Mesozoic led to deposits of sedimentary material that was relatively thinner atop the Wet Mountains such that AFT dates were not reset. As the Laramide Orogeny took place, the Sangre de Cristos and Wet Mountains were elevated due to thrust faulting. Synorogenic fill then began to even out the landscape. Assuming a near-level topography at the Eocene RMES (Figure 13d), all areas in this region would have been at the same elevation around 50 Ma. Once Oligo-Miocene exhumation was triggered, the sedimentary material of the Sangre de Cristo Mountains, Raton Basin, and Denver Basin began eroding at much faster rates than the Wet Mountains. While the basins experienced kilometers of vertical erosion, the basement rock had close to no loss. Eventually, basins would reach the current level they are at now, leaving ~1.6 km relief between them and the Wet Mountains. It is also likely that this massive loss of sedimentary material led to local isostatic rebound of the Precambrian peninsula, further contributing to the elevation seen in the Wet Mountains.

To further support that minimal erosion occurred in the Precambrian basement, the Greenhorn Mountain lava flow now sits at an elevation of ~3750m, 2km above the Raton Basin 30km east. This would suggest that since its emplacement at 34 Ma, sedimentary basins around it have formed km-scale relief while erosion on Greenhorn Mountain has nearly completely stopped.

The fact that the Sangre de Cristos are currently at a higher elevation than the Wet Mountains seems to contradict the erodibility argument, as one may expect them to be eroded down closer to the level of the Raton and Denver Basins. However, when focusing on AFT and AHe dates (Lindsey et al., 1986 and Ricketts et al., 2015 respectively), they support exhumation of the Sangre de Cristos continued throughout the Miocene. The elevation on this range can be explained by two factors. First, Laramide thrusting meant that material of the Sangre de Cristos were stacked much higher than both the basins and Wet Mountains. Secondly, these Paleozoic sequences are older than basin fill, allowing for greater lithification and increased resistance.

The difference between the resistant rock of the Wet Mountains and the sedimentary lithologies around them show the importance of considering erodibility potential in one's region of interest, as this can greatly influence the recorded thermochronologic dates and subsequent interpretations. To best determine the rates of exhumation, the material with the greatest potential of erosion should be studied as these most accurately match the timing of initiation (Flowers & Ehlers, 2018). With nearly 2km of height in the Wet Mountains, this range would not exist had it not been for minimal erosion of its body, kilometers of erosion around its edges, and isostatic compensation.

In Flowers & Ehlers (2018), thermochronology done on crystalline rocks record earlier exhumation dates in the Front Range, to the north of our study area. This could suggest that the exhumation event affecting the Southeast may not have occurred to the north of Colorado, or that the majority basement coverage in the Front Range meant it was simply not recorded successfully. To best compare these two regions, other igneous rocks exposed within sedimentary sequences should be targeted in the Front Range, similar to the setting of the Spanish Peaks (see Section 6.2).

5. 2. Cenozoic Exhumation in the Southeastern Colorado Rockies, Northeast New Mexico and the Great Plains

Chapter 4 of Landman (2016) details the timing of Cenozoic exhumation along a proposed north-south transect at the western edge of the Great Plains. Running from the Spanish Peaks, CO in the north, to Capitan Pluton, NM in the south, the ~400 km transect was concluded to have a south-to-north pattern of exhumation. Low-temperature apatite (U-Th)/He dates were found to be older at the southern extent (Capitan Pluton), with erosion occurring at around 30-25 Ma. Southeast Colorado was inferred to have been exhumed later due to AHe dates ranging from 23-11 Ma (Landman, 2016). While these locations show evidence that would support a northward-moving pattern of exhumation, the large distance between the two leave opportunities to study if this event was continuous throughout central and northeast New Mexico.

This section describes the addition of low-temperature thermochronology dates in and around these regions to better understand the timing and spatial trends of exhumation. Building off the work from Landman (2016), I aim to expand these patterns in three ways: (1) By extending dates to lower elevations around the Spanish Peaks, (2) by filling in the gap between the Spanish Peaks and Capitan Pluton through analysis on the Chico Hills, NM, and (3) by looking east into the Great Plains (Figure 1).

The dates found by Landman (2016) are detailed below (Section 5.2.4). Once all areas of interest have been discussed, regional patterns will be identified, followed by potential causes of exhumation observed.
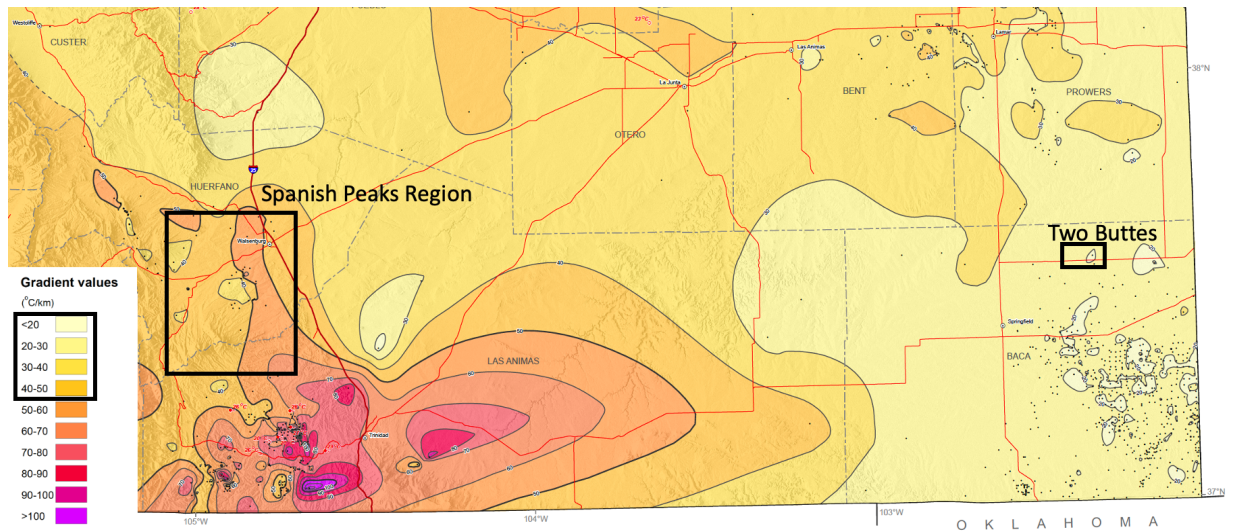

Figure 14: Modified from Berkman & Watterson (2010). Geothermal gradient contours of Southeast Colorado. Black boxes show locations of low-temp thermochronology dates from this study and their associated geothermal gradients.
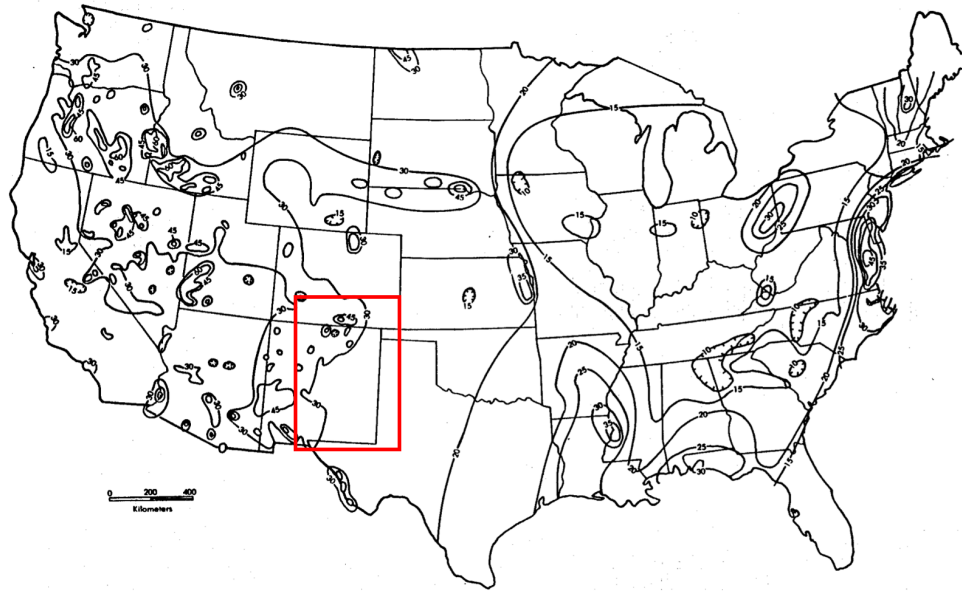
Figure 15: Geothermal gradient map of the United States. Contour interval is 15°C/km in the western U.S. and 5°C/km in the eastern U.S. Red box indicated study area. Modified from Kron et al., 1980.
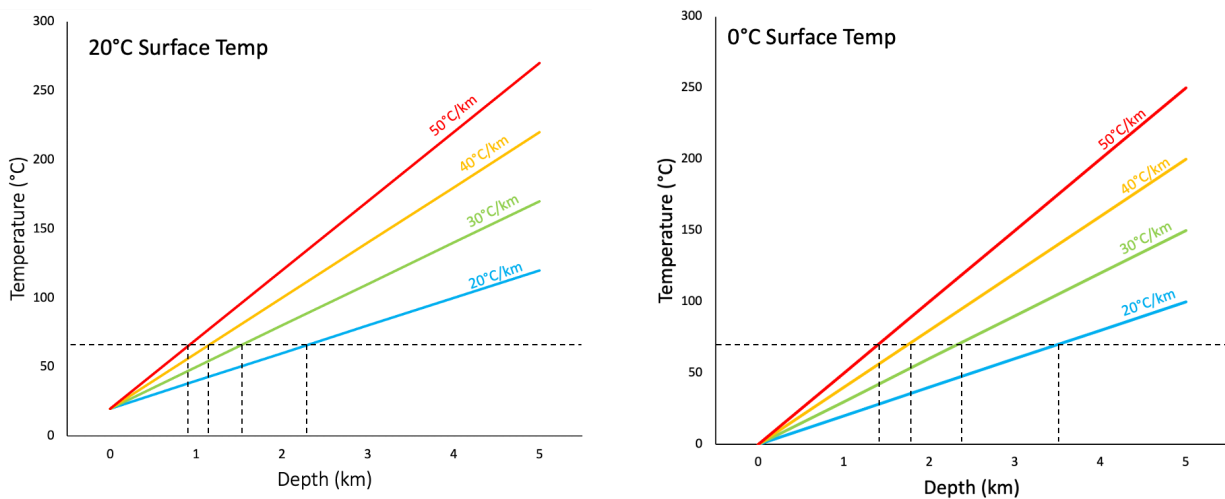

Figure 16: Temperature-depth profiles with different geothermal gradients assuming a surface temperature of 20°C and 0°C respectively. Geothermal gradients for the study region are taken from Berkman & Watterson (2010). Spanish Peaks region at 40-50°C/km, Two Buttes at 20-30°C/km. Dashed lines represent the closure temperature of apatite (70°C) and the depth at which the rock would have passed through this depending on the geothermal gradient.

To estimate rates of exhumation, the differences in depth-temperature profiles between study areas must be considered. The Spanish Peaks Region which includes the Spanish Peaks and Huerfano Butte show geothermal gradients of 40-50°C/km, whereas Two Buttes to the east has values around 20-30°C/km (Figure 14) (Berkman & Watterson, 2010). The Chico Hills and most of New Mexico's Great Plains have a gradient of ~20-30°C/km (Figure 15) (Kron et al., 1980). This affects interpretations of the amount of overlying material when the thermochronometer passes through its closure temperature. A

24

higher geothermal gradient means an apatite mineral will pass through 70°C at shallower depths, whereas lower gradients will reach the same temperature deeper into the lithosphere (Figure 16).

5. 2. 1 Exhumation in South-central Colorado: The Spanish Peaks Region

As described in section 5.1, the Rocky Mountains of South-central Colorado have had a long history of thermochronology studies centered around ranges such as the Sangre de Cristos and the Wet Mountains. Landman (2016) conducted AHe work on the Spanish Peaks in the Raton Basin (Figure 17) to form a vertical transect of over 900m. CS13-1 was the lowest elevation sample from this data set at 2054m. However, while the other 3 samples from Landman (2016) are located along the East Spanish Peak pluton, CS13-1 is ~30 km to the north in the Little Black Hills (Figure 17). To better see exhumation rates, 2020 sampling of a radial dike from the base of the Spanish Peaks (SK20-1) gave a closer 'low-elevation' data point.
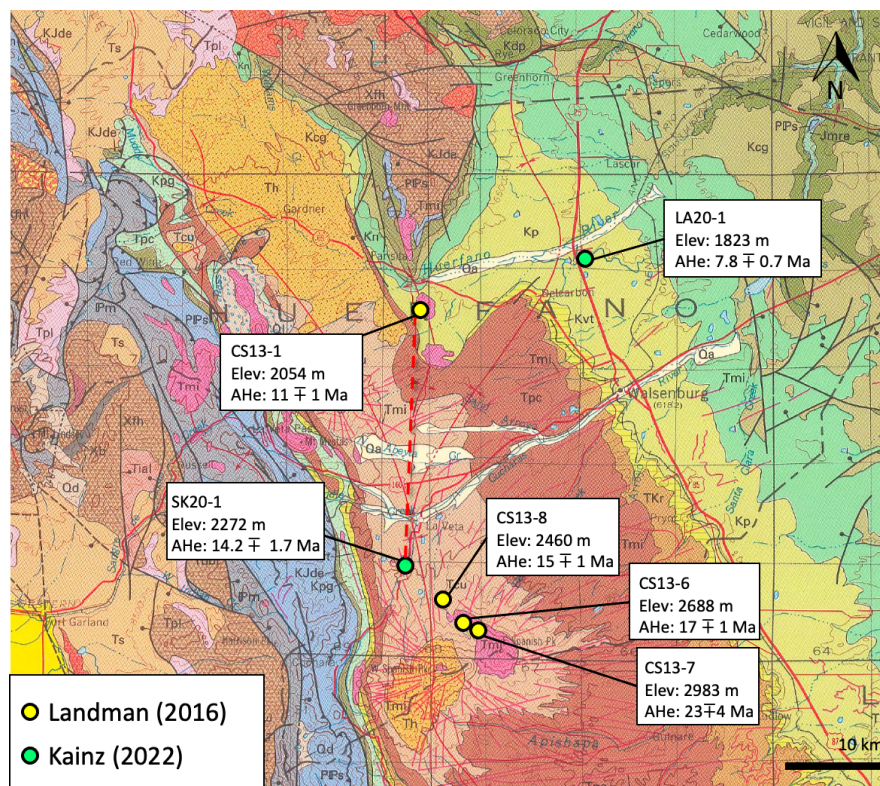

Figure 17: Sample map from the Spanish Peaks Region of South-central Colorado. Base map modified from Tweto (1979).

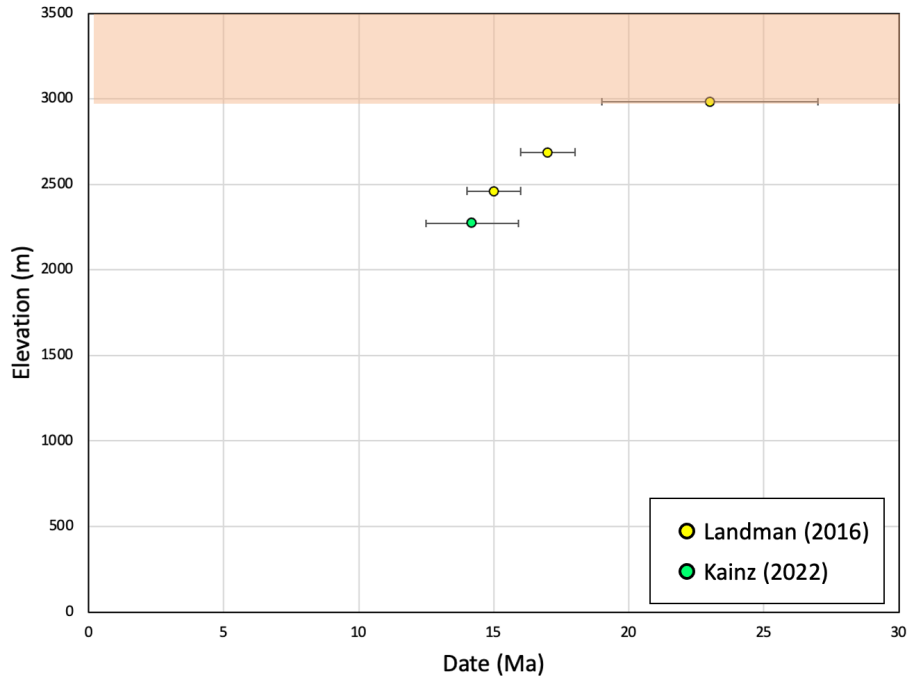Figure 18: Vertical profile of AHe dates along East Spanish Peak. Beige box at ~2900m+ represents elevations recording emplacement rather than exhumation. This is inferred from the highest elevation AHe date being very similar to pluton emplacement age (23.9±0.08 Ma $^{40}Ar/^{39}Ar$) (Penn & Lindsey, 2009). Therefore, any elevation shallower than these record cooling to below 70°C (1-3 km depth) at emplacement.
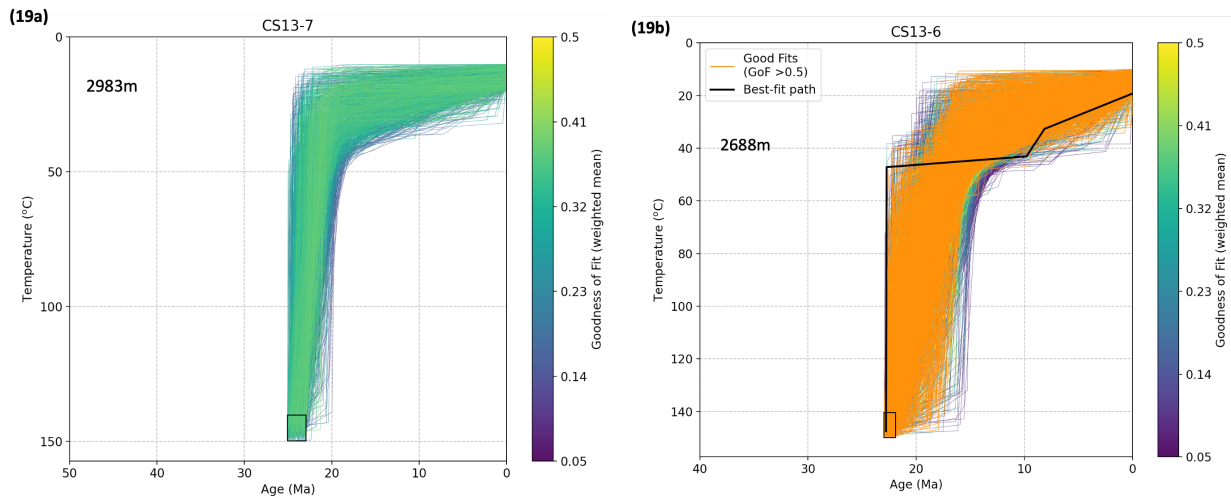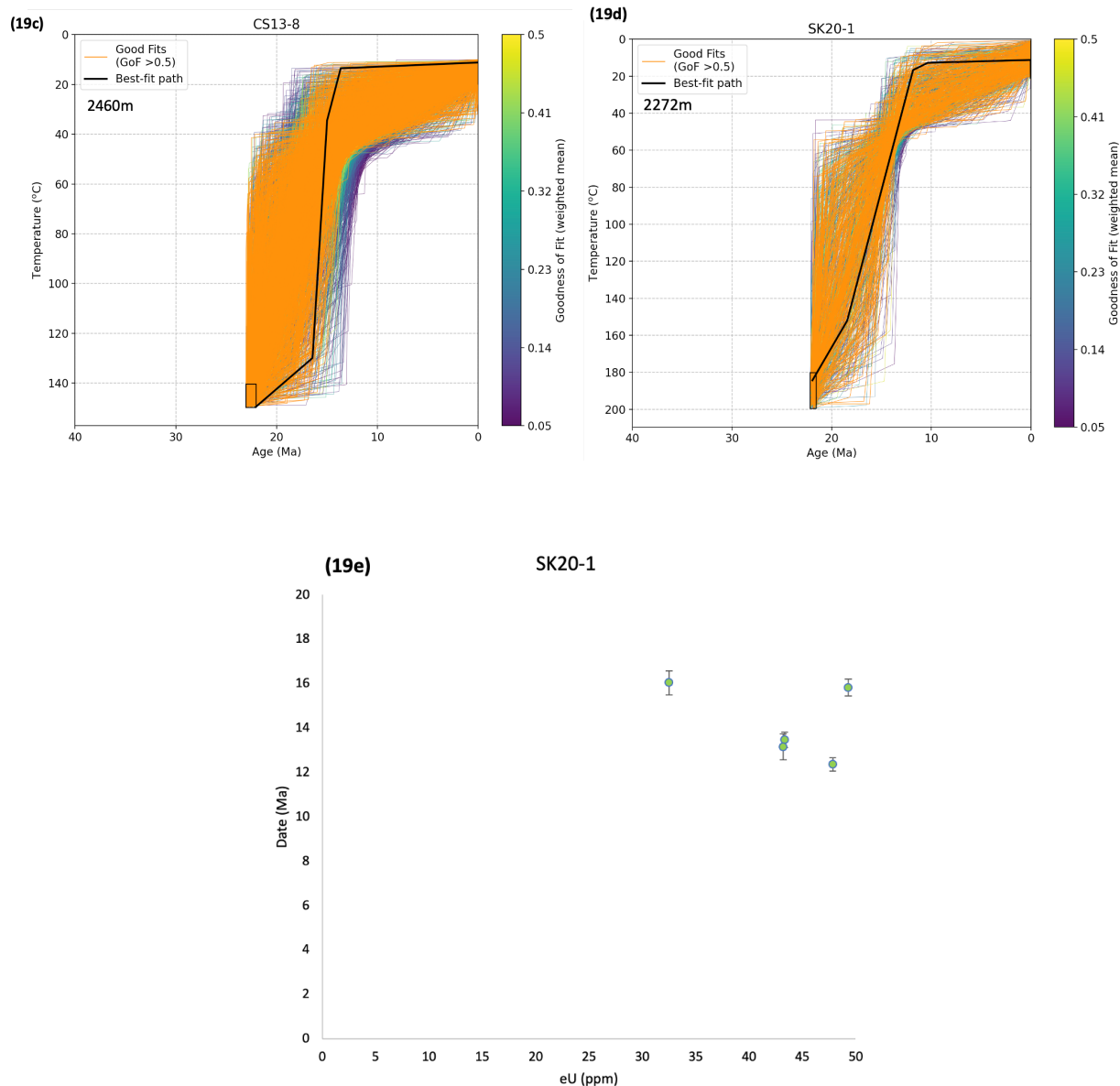
Figure 19a-e: HeFTy plots for the Spanish Peaks (19a) CS13-7; (19b) CS13-6; (19c) CS13-8; (19d) SK20-1; (19e) date-eU for SK20-1

Data combined from my 2020 campaign and Landman (2016) showed AHe dates from 23-14.2 Ma, indicating these samples cooled through ~70°C during the Miocene. Figure 18 shows a positive slope of elevation against age, from which a rough estimate of rates of cooling occurred. $^{40}Ar/^{39}Ar$ ages put the formation of East Spanish Peak at 23.9 ± 0.08 Ma (Penn & Lindsey, 2009), which is very similar to Landman's (2016) highest elevation AHe date, CS13-7, at 23 ± 4 Ma. Because of this, we interpret elevations above this sample to be recording emplacement rather than exhumation, as they were likely shallower than 1-3 km at the time of emplacement (and therefore cooled immediately below ~70°C). The three low elevation samples on the Spanish Peaks vertical transect then show AHe dates from 17-14 Ma, which corresponds to a rate of exhumation of ~130m/m.y. HeFTy plots of all 4 samples show the possible thermal paths for samples at each elevation using inverse thermal history modeling (Ketcham, 2005) (Figures 19a-d).
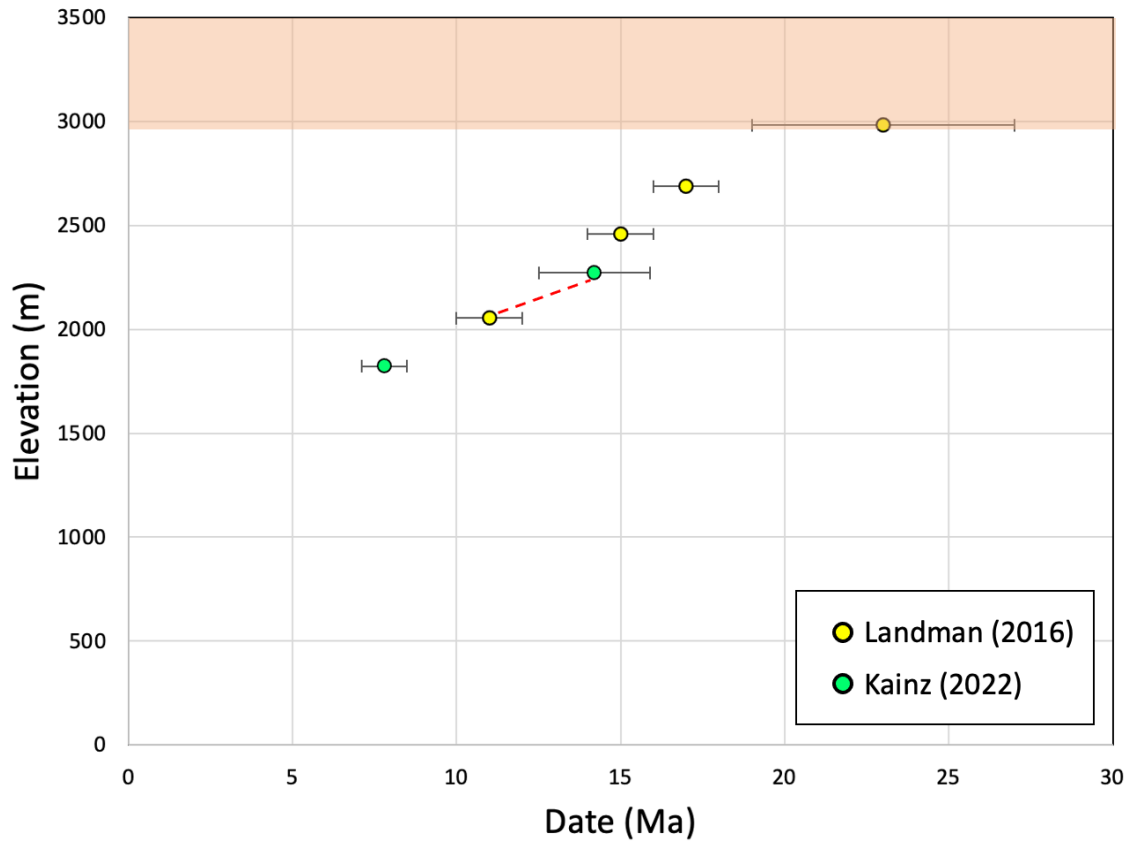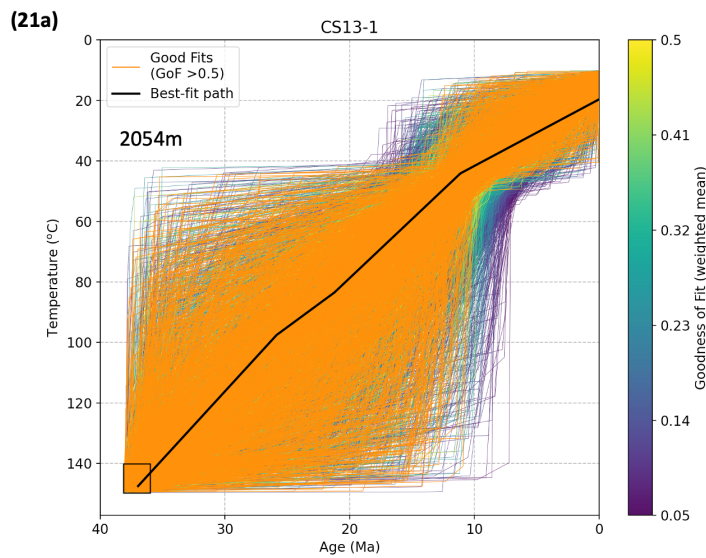
Figure 20: Combined pseudo-vertical transect from the whole Spanish Peaks region. The two lowest elevation samples are located ~30km north of the Spanish Peaks transect. Beige box at ~3000m+ represents the modern elevations that were once shallow enough to record emplacement rather than exhumation.
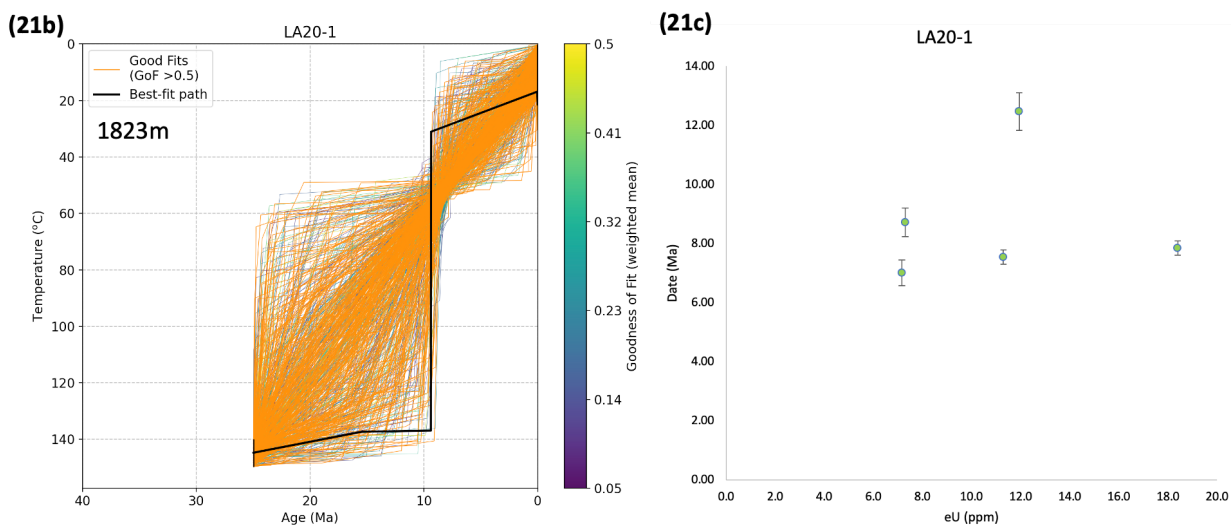
Figure 21a-c: (21a) HeFTy inverse thermal model for CS13-1 in the Little Black Hills; (21b) Hefty model for Huerfano Butte (LA20-1); (21c) date-eU trends for LA20-1.

Though the Spanish Peaks vertical transect (Figure 18) shows an inferred rapid exhumation beginning at around 17 Ma, this is only recorded for 5 Myr. To determine whether this continued at lower elevations, we can look north towards the Little Black Hills and Huerfano Butte (CS13-1 and LA20-1 respectively). Huerfano Butte stands at ~1800m with an AHe date of 7.8∓0.7 Ma. Emplaced at 25 Ma (Penn & Lindsey, 2009), it was likely intruded to a depth of around 2 km (Litton, 2020).

Although these lower elevation dates do not continue the vertical transect due to being too far apart spatially, they do suggest that exhumation was continuing regionally until 8 Ma. Combining all data from this region creates a pseudo-transect that would indicate an erosion rate of roughly 100m/m.y (Figure 20).

Date-eU plots from SK20-1 and LA20-1 both show small spreads and no strong positive correlation, indicating fairly quick and simple cooling (Figures 19d & 21b respectively). The outlier of LA20-1 (a02) has an older date of 12.5 Ma compared to the other aliquots, and was excluded from HeFTy thermal modeling. Justification for its omission was due to a low alpha ejection factor (Ft) of 0.686 on the grain (see Results). While this is not less than the 0.65 Ft cutoff, it is still anomalously low.

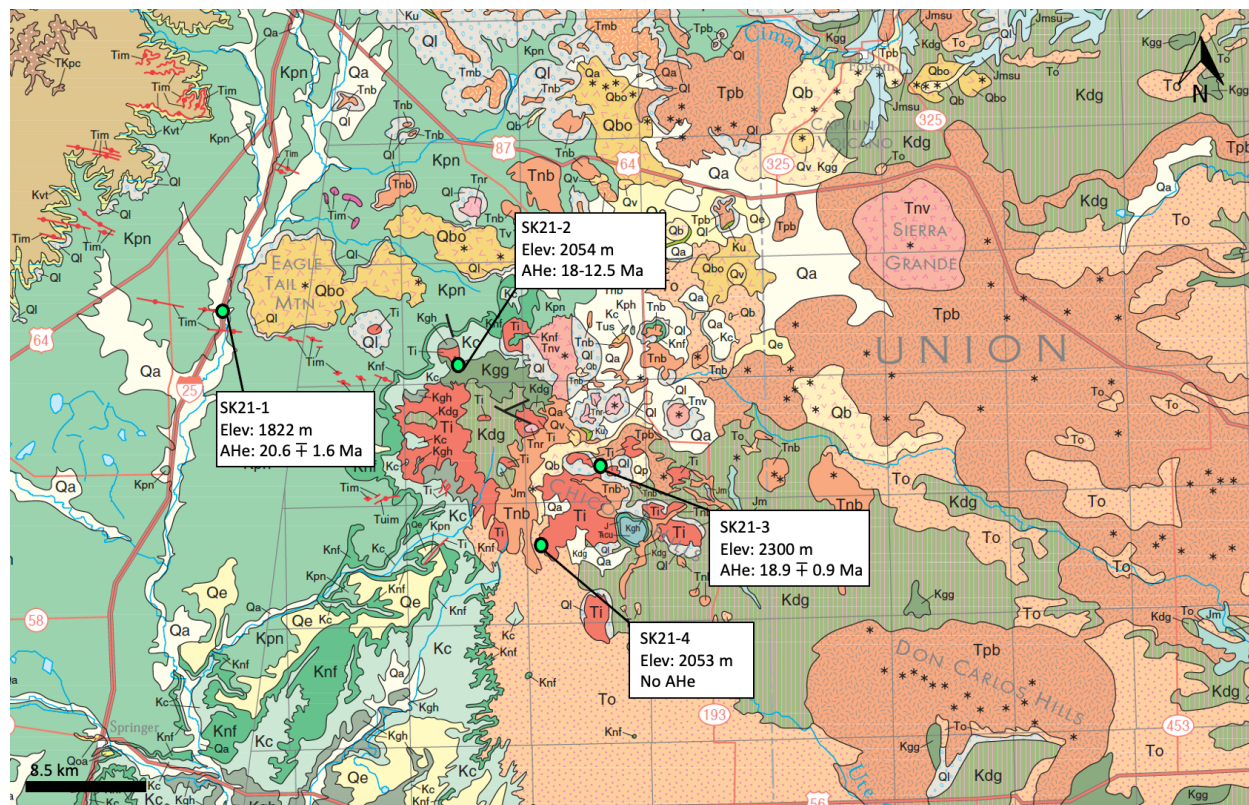### 5. 2. 2. Exhumation in the Chico Hills, New Mexico

Figure 22: AHe dates for Chico Hills samples in New Mexico. Note the Ogallala Formation (To) surrounds SK21-3.

The Chico Hills Sill Complex in Colfax County, New Mexico, contains many Cenozoic igneous rocks scattered throughout Cretaceous sedimentary material. Both volcanic and shallow plutonic bodies are found here, dated via K-Ar to range from 37-5 Ma (Scott, Wilcox & Mehnert, 1990). Emplacement ages on these indicate the area was subject to multiple volcanic episodes since the Laramide uplift. These include volcanism from the Ignimbrite Flare-up, Rio Grande Rift, and Jemez Lineament. The exhumation event of interest is expected to have predated Jemez volcanic activity, and thus bodies with pre-Miocene K-Ar ages were targeted. Concerns with resetting of AHe ages from Jemez volcanism are addressed in the uncertainties and errors section.

Four intrusive bodies were chosen: the Eagle Rock Dike lamprophyre (SK21-1), the Laughlin Road Slagle Trachyte sill (SK21-2), the Piney Mountain Road tephrite (SK21-3) and another Tertiary sill (SK21-4) (Figure 22). Emplacement ages for the Eagle Rock Dike were set at 24.16 ∓ 1.04 Ma via K/Ar (Scott, Wilcox & Mehnert, 1990). SK21-2, the Slagle Trachyte, is the oldest dated igneous body in the Chico Hills at 36.7 ∓ 1.3 Ma (Staatz, 1985). SK21-3 only has inferred ages from geologic relationships in the area that put its formation between the Slagle Trachyte and the 25 Ma Chico phonolite (Scott, Wilcox, & Mehnert, 1990). Therefore, the emplacement age of SK21-3 is between 37-25 Ma. SK21-4 was an ideal target because of its spatial relationship with the Ogallala Formation. Ogallala deposits directly adjacent to the sill tell us that it must have been exhumed by the time the unit was forming. Fossil and detrital zircon U-Pb ages put the start of Ogallala deposition at anywhere from 12.5-9 Ma in this region (Smith et al., 2016; Zakrzewski, 1988; Tedford et al., 2004). Lack of appropriate apatite grains from SK21-4 meant (U-Th)/He analysis was not carried out on this sample.
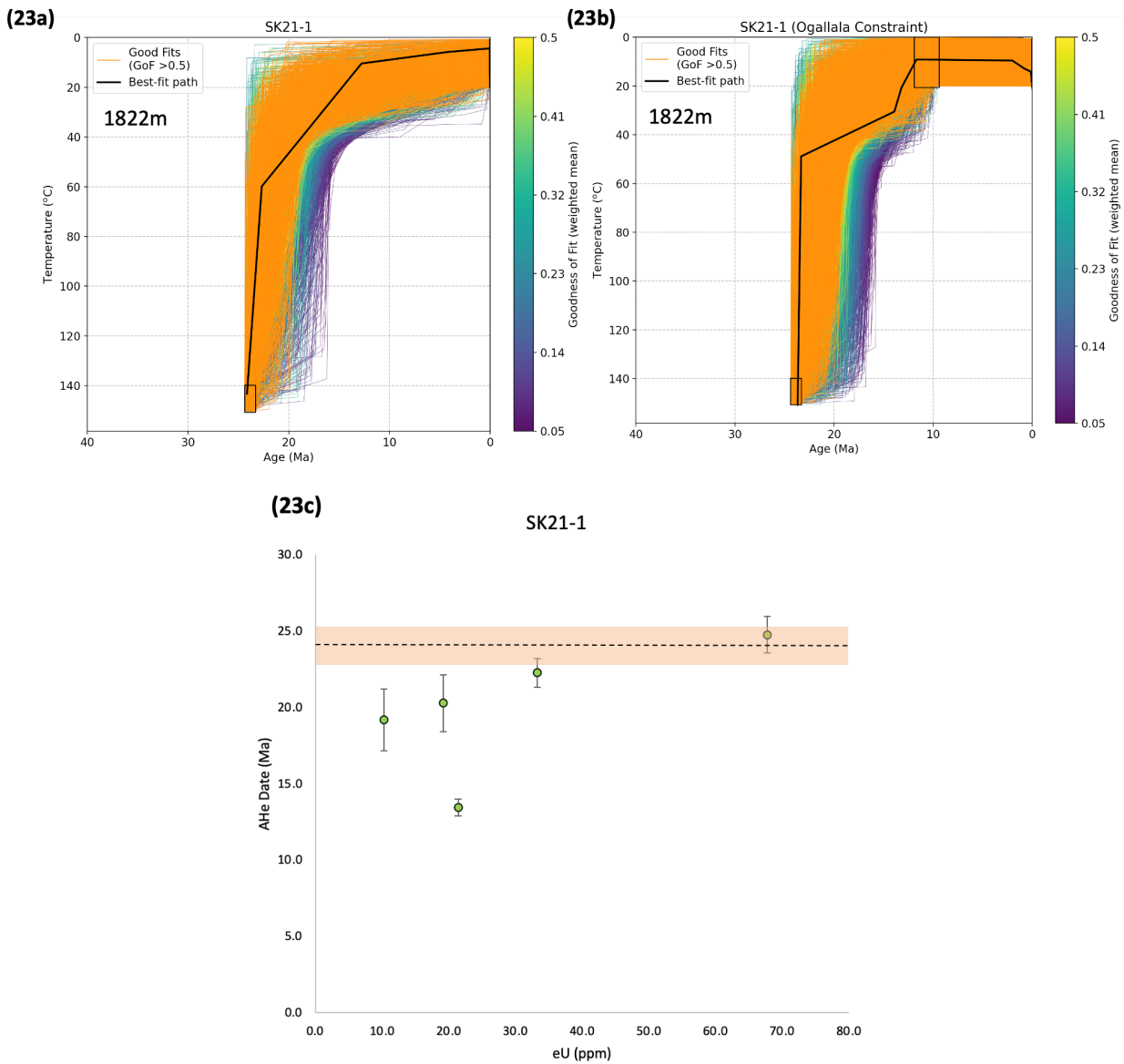
Figure 23a-c: (23a) HeFTy thermal model for Eagle Rock Dike (SK21-1); (23b) HeFTy thermal model for SK21-1 with Ogallala surface constraint; (23c) Date-eU plot for SK21-1. Beige zone is emplacement.

AHe dates from the three measured samples are between 24-13 Ma from individual grain dates, suggesting exhumation was taking place in the first half of the Miocene. Date-eU from Eagle Rock Dike, SK21-1 (Figure 23c), shows a fairly large spread of eU dates that have a rough positive slope. The grain with a high eU (a04) at 68ppm provided a date at 24.8 ∓ 4 Ma, which is within emplacement age (24.16 ∓ 1 Ma (Scott, Wilcox, and Mehnert, 1990)). This grain was omitted from thermal modeling on the basis of it being too small (Ft = 0.55). The outlier with the youngest date (13 Ma) also was not put into thermal modeling due to uncertainty surrounding the grain shape. A large chip in grain SK21-1_a02 adds a lot of ambiguity to the determination of ^{4}He loss. This leaves three grains remaining which form a positive date-eU trend, that all yield dates younger than emplacement. Patterns like this are only likely to occur via exhumation being recorded as opposed to emplacement.

Omitting the aforementioned grains from the overall average, SK21-1 gives a date at 20.8 ∓ 1.6 Ma. Although other samples from this area were not in as close proximity to the Ogallala Formation as SK21-4, the abundance of the unit throughout the Chico Hills provides substantial evidence to put many of these igneous rocks at the surface during its deposition. Figures 23a and 23b show thermal models without and with the Ogallala surface constraint respectively for Eagle Rock Dike. Even if the dike was on the surface by 12-9.5 Ma, this would not affect the older thermal history. Both models suggest the most rapid period of cooling was around 24-17 Ma.

HeFTy plots have many 'good' fits that cool to the surface at emplacement, which leads to uncertainty as to the event recorded by these dates. If emplaced shallowly enough, the rock would cool to below 70°C during its formation. However, when coupled with date-eU, the most plausible interpretation is that this is a signal of exhumation.
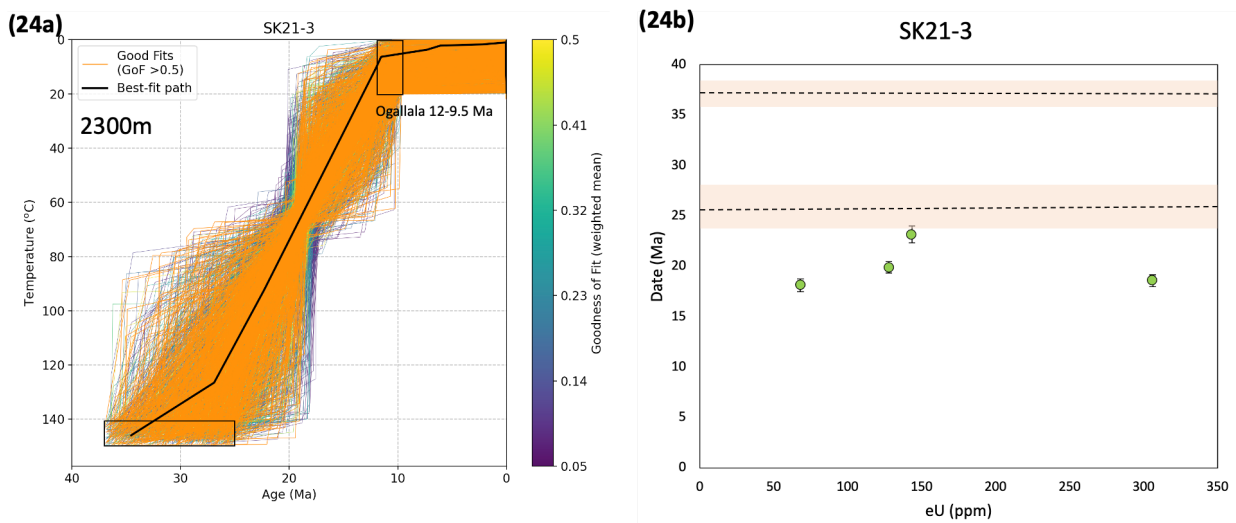

Figure 24a-b: (24a) HeFTy thermal model that assumes exposure at surface by 12-9.5 Ma due to Ogallala base deposition ages; (24b) Date-eU. Beige box represents the range of emplacement ages: older limit at 37 Ma by K/Ar (Staatz, 1985), younger limit at 25.8∓1 (Scott, Wilcox, and Mehnert, 1990).

SK21-3, the Piney Mountain Road Tephrite, yielded an AHe range of 24-18 Ma from individual grain dates. The younger limit of inferred emplacement ages (25.8 ∓ 1 Ma (Scott, Wilcox, & Mehnert, 1990)) overlaps with the oldest AHe date, but its average, as well as the rest of the grains, fall below emplacement with good agreement to one another (Figure 24b), indicating they record later erosion. If it were intruded to a depth that correlated with <70°C, AHe dates would be equivalent to emplacement ages.

Thermal modeling for the tephrite is consistent with relatively simple cooling histories, none of which suggest cooling below 70°C at emplacement. All good-fit paths show the sample staying hotter than 60°C until 21 Ma, 4 m.y. after the youngest possible emplacement time. With this in mind, all paths suggest this is representative of an exhumation event.

Endmember paths for SK21-3 using HeFTy modeling (Figure 24a) suggest either (1) that the area sat at depth for 5-25 m.y. before rapid cooling to the surface at 12 Ma, or (2) that there were two significant periods of exhumation with the rock sitting at 60-80°C for ~10-25 m.y. in between. The larger age estimates on these cooling pathways are due to uncertainty of the emplacement age of the intrusion.

Exhumation amounts were calculated assuming a geothermal gradient of 20-30°C/km (Kron et al., 1980), consistent with 470-190 m/m.y. Although the intrusion and Ogallala Formation are not exactly adjacent, the Ogallala is seen to the north, east and south, giving a stronger argument as to its position at the surface at 12-9.5 Ma (in contrast to Eagle Rock Dike where no Ogallala surrounds it).

(25a)

(25b)

(25c)
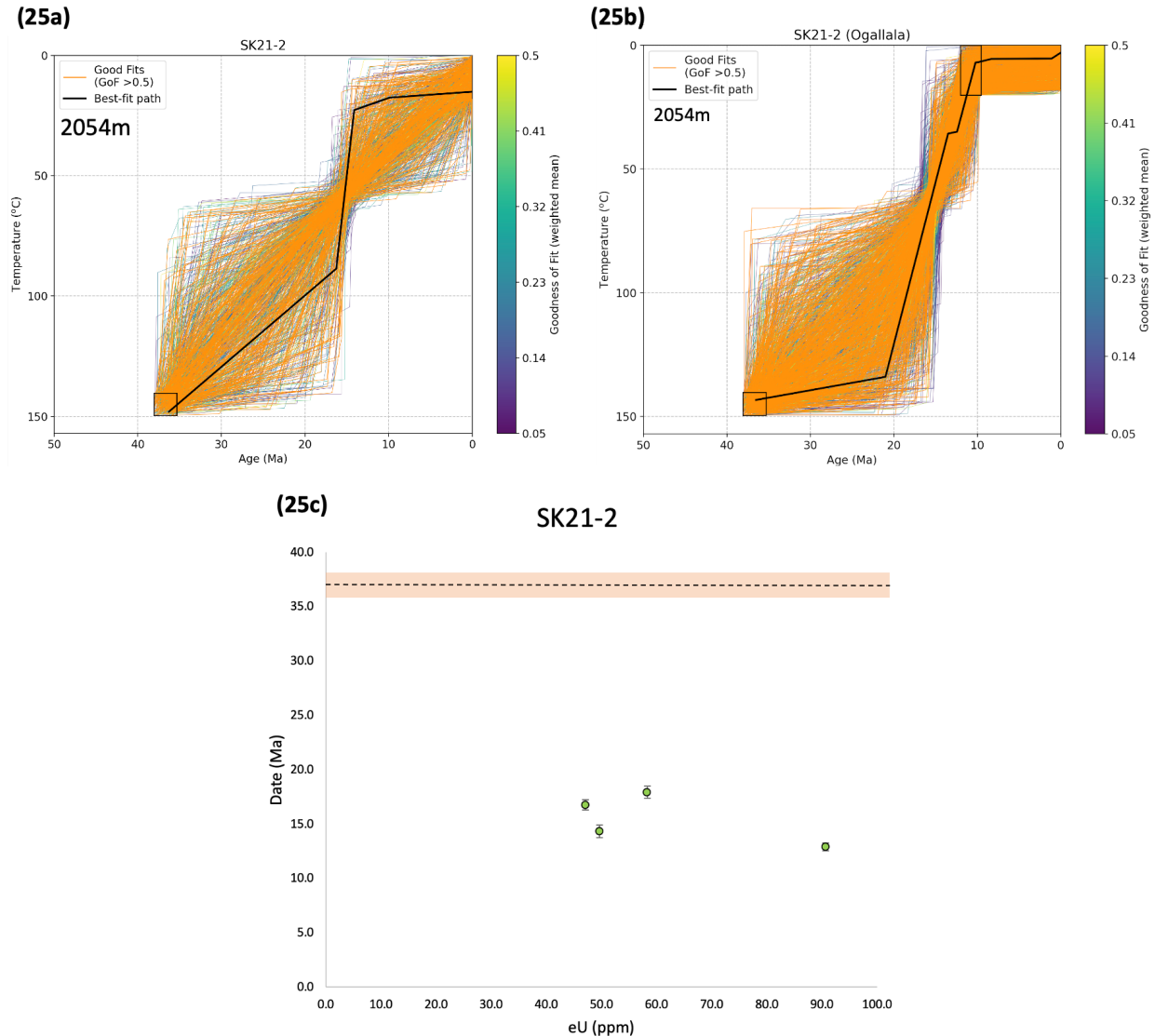
Figure 25a-c: (25a) HeFTy tT model for the Slagle Trachyte (SK21-2) without Ogallala constraint; (25b) HeFTy tT model for SK21-2 with Ogallala constraint; (25c) date-eU for SK21-2

While other samples from this area may hold uncertainty as to whether they are recording exhumation or not, SK21-2 has an established K/Ar date at 37 Ma (Staatz, 1985). AHe dates from this study range from 18-13 Ma, much younger than emplacement, making it unambiguous that these Miocene dates are from exhumation. Notably, these are consistent with dates from the aforementioned Chico Hills samples, leading to a strong argument that all record exhumation. A relatively flat date-eU implies a fairly fast cooling history, expected for a rock this young in age (Figure 25c).

Similar to SK21-1, the Ogallala is not completely surrounding SK21-2, so using it as a surface constraint is not as reliable as with SK21-3. Addition of this constraint (Figure 25b) does not change

much about the patterns of possible cooling pathways, other showing more 'good' fits supporting one rapid exhumation rather than two episodes.

There is strong evidence that the AHe dates in the Chico Hills are from our proposed Miocene exhumation rather than from emplacement or later Rio Grande Rift heating. While it is possible that heating from the Jemez Lineament did arch up the area (Leonard, 2002), this would have occurred after the deposition of the Ogallala Formation in the late Miocene. We do not deny the possibility of this happening in the Chico Hills, but rather that AHe sees past this and records an earlier event. The three describe samples agree when in conjunction with one another, suggesting these dates are likely to be from exhumation. This would mean that their rise to the surface took place from 22-13 Ma, which would have stopped 8 m.y. before the youngest South-central Colorado AHe dates (Huerfano Butte at 8 Ma).

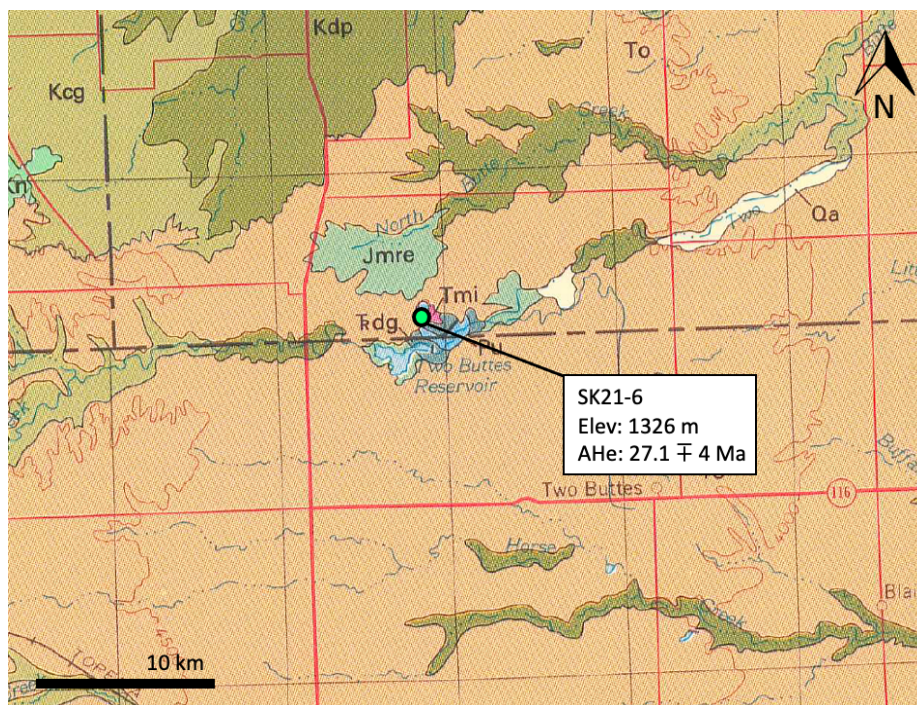## 5. 2. 3. Exhumation of the Great Plains at Two Buttes

Figure 26: AHe for the Two Buttes lamprophyres in the Two Buttes State Wildlife Area, Prowers County, CO; Note the Ogallala Formation (To) surrounding the area.

(27a) SK21-6

(27b) SK21-6 (AFT Constraint)

(27c) SK21-6
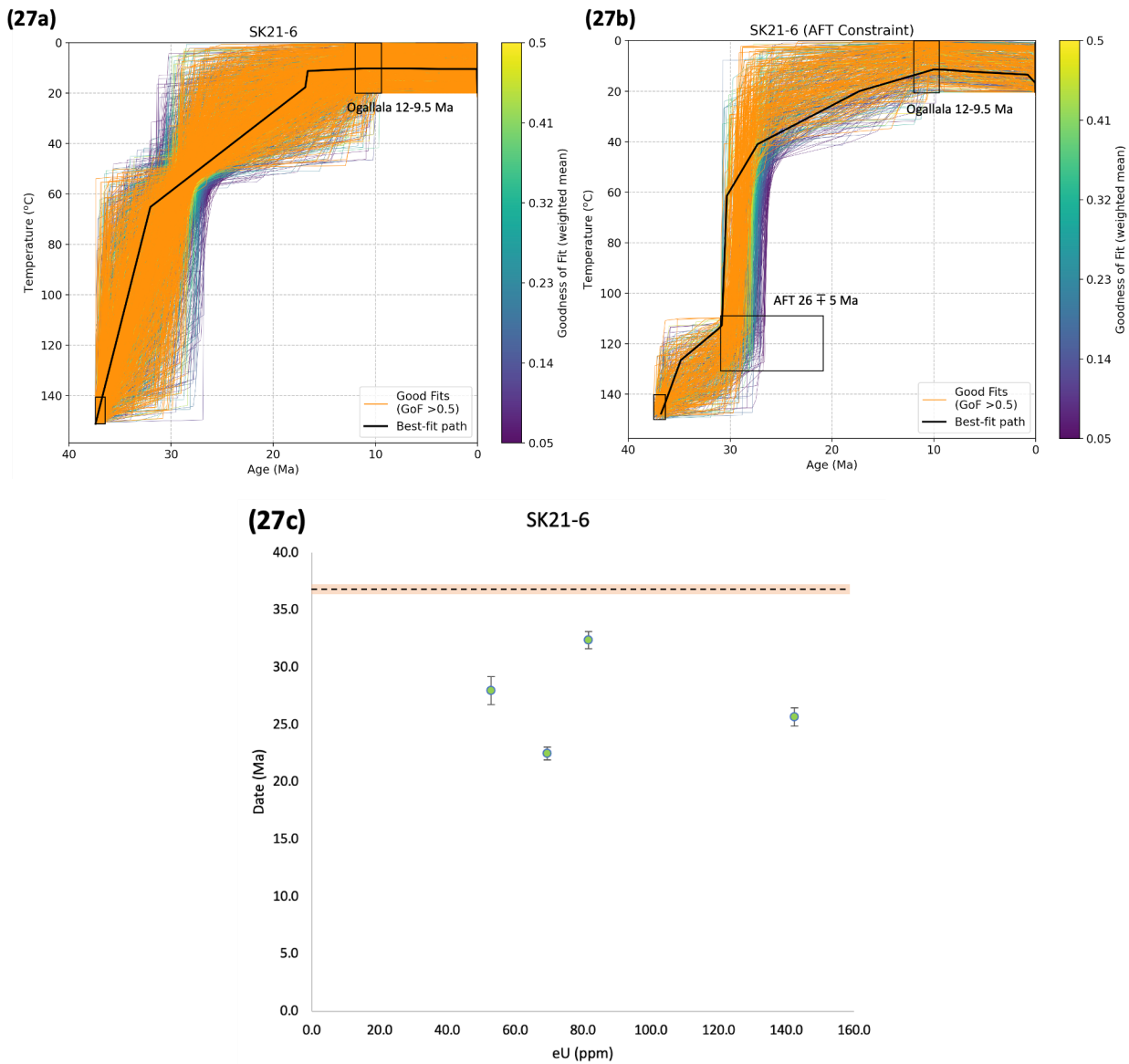
Figure 27a-c: (27a) HeFTy tT model for SK21-6 . Emplacement at 36.8 Ma ∓ 0.4 (Davis et al., 1996). Surface at 12-9.5 Ma from Ogallala constraint; (27b) HeFTy tT model for SK21-6 with AFT constraint box; (27c) Date-eU plot

The Two Buttes lamprophyres were sampled to determine if post-Laramide exhumation took place in the Great Plains, constraining the northeastern edge of the study area. Emplacement ages were found from K-Ar dating the complex back to 36.8 ∓ 0.4 Ma (Davis et al., 1996). From 4 apatite grains, an AHe date of 27.1 ∓ 4 Ma was calculated. The date-eU trend shows no strong correlation, but are all 5 m.y. younger than emplacement. Similar to SK21-3 (Chico Hills tephrite), eU concentrations are high (53-143 ppm).

Like in the Chico Hills, the Ogallala Formation is present near target igneous bodies. However, while the sampled rocks of the Chico Hills were further away from Ogallala deposits, they are adjacent to one another at Two Buttes, leading to less ambiguity of the timing when they were at the surface. Thermal modeling for SK21-6 is one of the better constrained plots from this study: Emplacement age, AHe, and surface exposure are all well constrained (Figure 27a).

A weak date-eU correlation makes it difficult to say much about rates of cooling. However, AFT at 25.7 ∓ 5 Ma represent closure temperatures of ~110-130°C (Pilione et al., 1977; Davis et al., 1996). Both AHe and AFT agree on exhumation occurring around 27 Ma, which would also suggest cooling through 70-130°C took place around the same time period (Figure 27b). This would put all 'good' fit pathways to rapidly cool below 70°C between 31-27 Ma, a relatively tight interval at when exhumation could have taken place. This amount of exhumation is much smaller than the km-scale erosion taking place in the Chico Hills at 20-12 Ma. Additionally, both the Chico Hills and Two Buttes are intruded into Cretaceous age sediments at similar stratigraphic levels. This would suggest that similar amounts of rock have been removed from both places, but this would have occurred later in the Chico Hills.

It is important to note that the AFT date was from 1977, a time at which low-temperature thermochronology was less calibrated. Thus, the date taken from this study should be taken with caution (James Metcalf, 2022, personal communication). Without this constraint, a greater number of possible t-T pathways indicate cooling as early as 37 Ma (Figure 27a).

Dates and modeling for Two Buttes implies post-Laramide exhumation also took place in the Great Plains. Rather than being of Miocene age, like in south-central Colorado and the Chico Hills, this took place nearly 10-20 m.y. prior, during the Oligocene. At over 100 km to the east of other sites of interest, regional patterns of exhumation begin to fall into place.

5.2.4. Exhumation in Central and Southern New Mexico

Low-temperature thermochronology from Landman (2016) provides the basis upon which this study was built. AHe from the Spanish Peaks region has already been detailed in section 5.2.1. More AHe and AFT from Landman (2016) provides a picture of exhumation taking place in eastern-central New Mexico, allowing us to understand if timing and rates to the south are comparable to aforementioned locations.
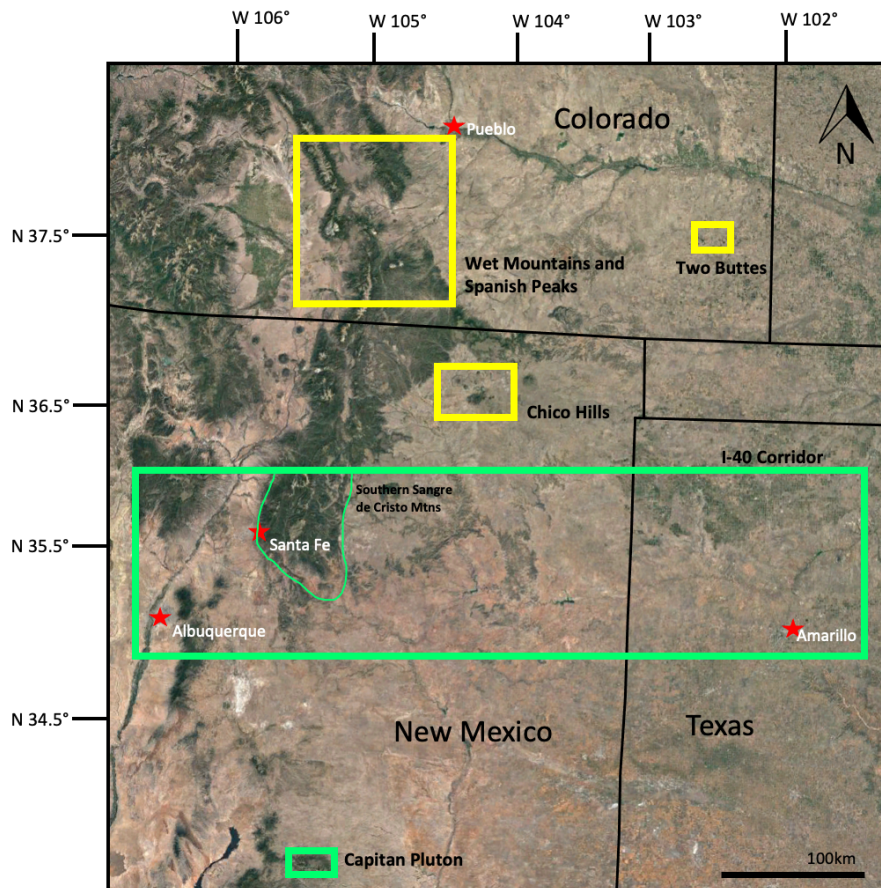
Figure 28: Green boxes represent locations of low-temperature thermochronology from Landman (2016).

5.2.4.1. Capitan Pluton, New Mexico
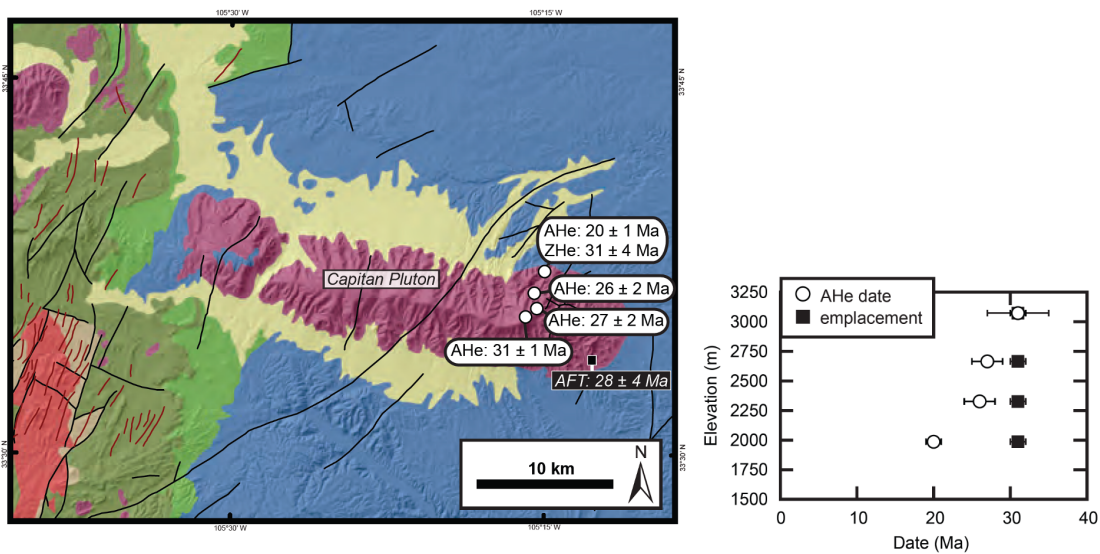
Figure 29: AHe at Capitan Pluton in Southeast New Mexico from Landman (2016).
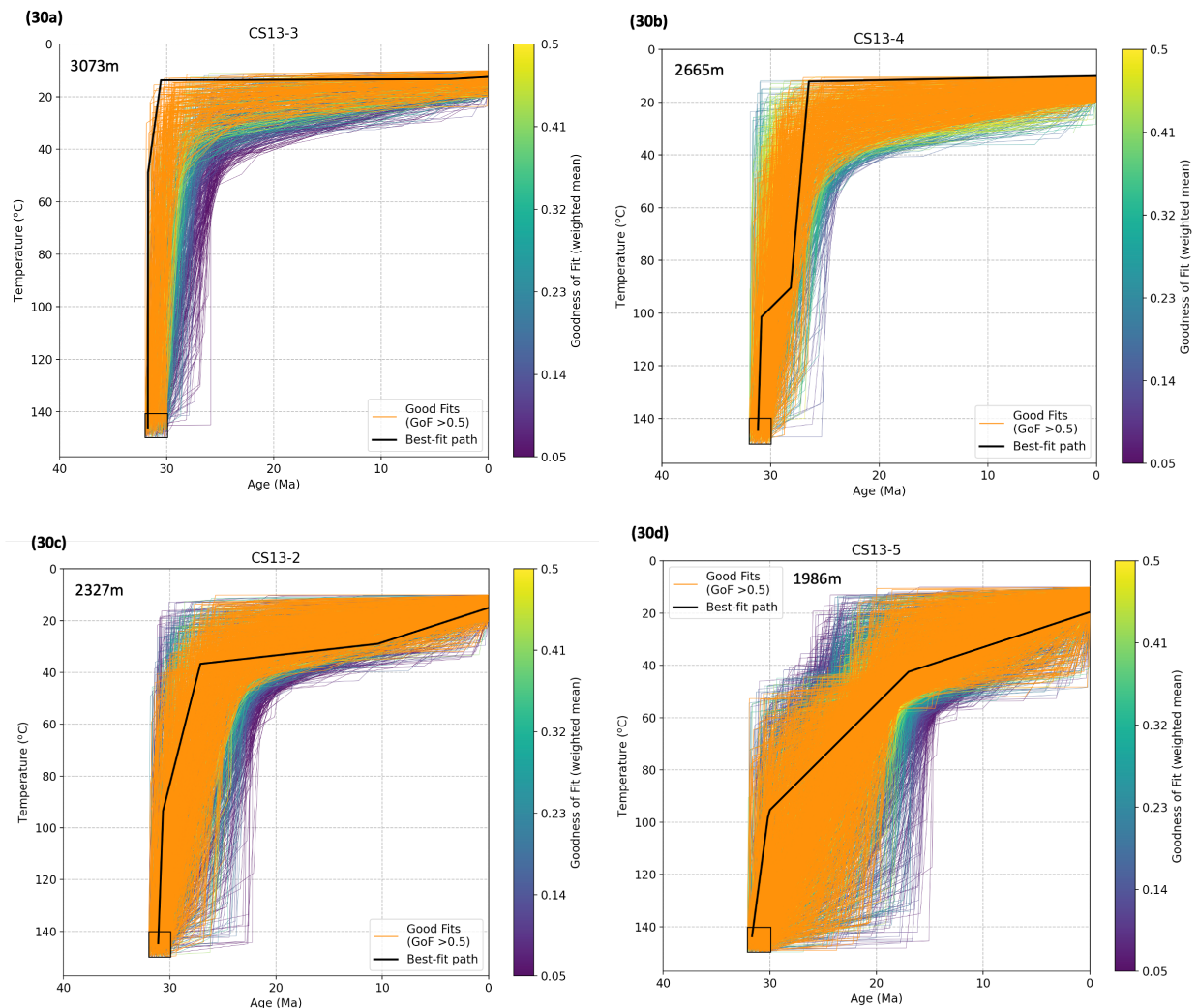
Figure 30a-d: HeFTy inverse thermal models for Capitan Pluton, New Mexico

Figure 29 shows the locations of AHe dates from Capitan Pluton in southern New Mexico. In a similar vein to the Spanish Peaks transect, ~ 400km to the north, the highest elevation sample is the same age as emplacement (31 Ma), suggesting that elevations above ~3000m were all intruded shallower than 1.5km. Cooling of lower samples again show around 1km of exhumation over 5 m.y. (Landman, 2016).

The amounts and rates of exhumation are of similar scale in both areas. However, the key difference between here and the Spanish Peaks is timing of exhumation. Oligocene dates at Capitan Pluton led Landman (2016) to conclude a south-to-north trend, where a continuous exhumation event first was captured in southern New Mexico before moving towards southern Colorado. Overlap with the propagation of the Rio Grande Rift and Ignimbrite Flare-up volcanism led Landman (2016) to explain this pattern to surface uplift epeirogeny.

HeFTy thermal modeling agrees with these interpretations. The highest elevation sample (Figure 30a) cools to surface temperature immediately upon emplacement, whereas lower samples show later cooling below 70°C (Figure 30b-d).

5.2.4.2. The Southern Sangre de Cristo Mountains and the I-40 Corridor of New Mexico

Figure 31: (A) Geologic map of the Southern Sangre de Cristo mountains with sampling locations, and AFT & AHe dates. (B) Schematic cross section of the region. (Landman, 2016 (adapted from Baltz & Myers, 1999; Koning et al., 2013)). Color outlines represent low-temperature thermochronology dates of respective ranges within the Sangre de Cristos. Adapted from Landman (2016).
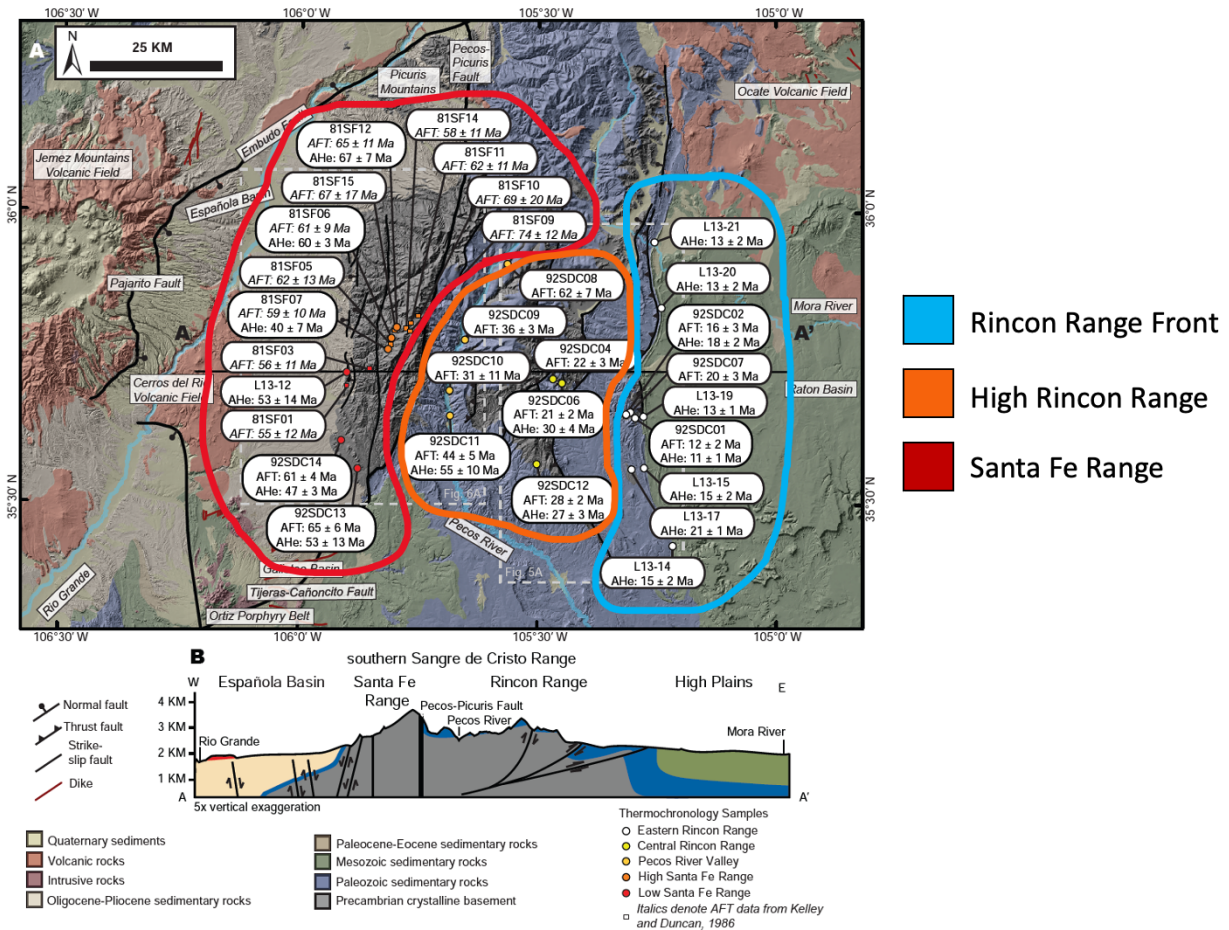
AFT and AHe collected in the Southern Sangre de Cristo range of New Mexico show three distinct date distributions that coincide with the location at which they were measured. The High Rincon Range (Figure 31) dates to the Oligocene-early Miocene. Just west, in the Santa Fe Range, timing is significantly older with dates from the Eocene to as far back as the Late Cretaceous. Another key aspect to note is that the age difference between AFT (~3.5km depth) and AHe (~1.5km depth) is as large as 20 m.y., suggesting that exhumation was much slower. Finally, at the Rincon Range Front to the east, dates are all mid-Miocene, similar to timing in the Spanish Peaks. Here, AFT and AHe are no more than 5 m.y. apart, showing a stark contrast to the slow exhumation 50km west.

Landman (2016) proposes each range records a separate event. The Santa Fe Range, isolated to the west by the Pecos-Picuris Fault, records Laramide uplift. The High Rincon Range is from extensional deformation during the Oligocene. Finally, the Rincon Range Front is from a more ambiguous mid-Miocene exhumation. The tentative conclusion was that this was the erosion signal brought about by the mid-Miocene Climate Optimum, beginning around 15 Ma (Zachos et al., 2001). Warmer temperatures and increased precipitation would have enhanced denudation. However, Landman (2016) notes that this

climate change would not explain erosion patterns that took place below the Ogallala Formation. Instead, we suggest that this Miocene exhumation can better be understood by an epeirogeny (see Section 5.2.7). This event is the same as that recorded in the Spanish Peaks, Chico Hill, Capitan Pluton, and Two Buttes.

It is also important to note that the Santa Fe Range is composed of Precambrian basement, whereas the Rincon Range is made of Paleozoic sedimentary rocks. Harking back to Section 5.1, it is possible that the large variability in dates of the Santa Fe Range are in part due to their greater resistance, resulting in older inferred erosion timing. Thus, newer exhumation events may not have been recorded in this range, but that does not mean they did not occur.
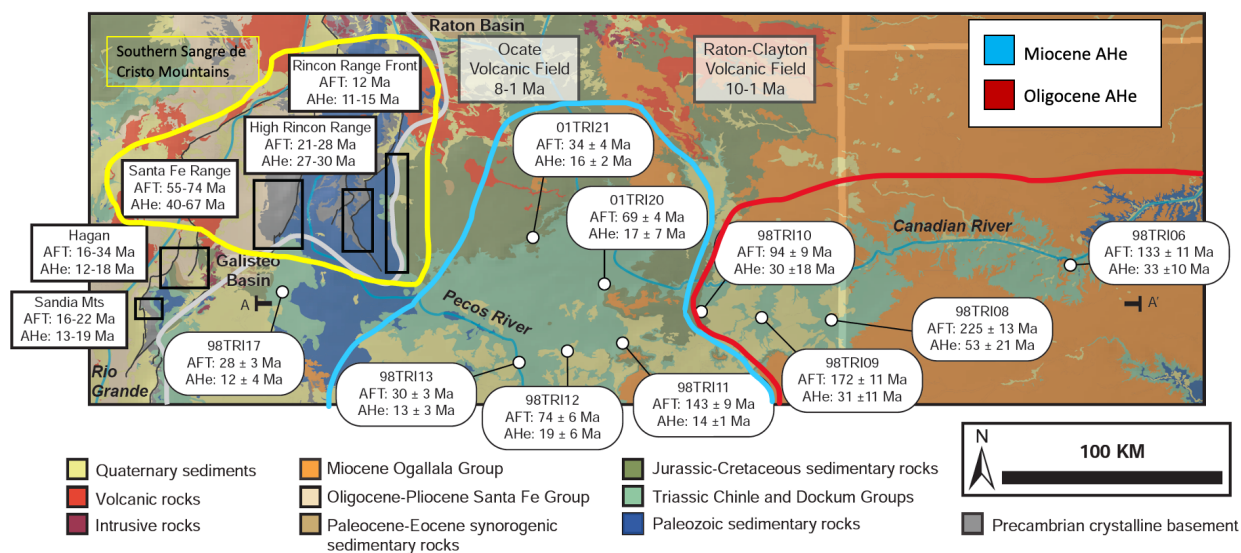

Figure 32: Sample transect of low-temperature thermochronology dates from Landman (2016). "The thick gray line marks the eastern front of the North American Cordillera. Data for the Sandia Mountains and Hagan Embayment are from House et al., 2003. Data for the Santa Fe Range is from Kelley & Duncan, 1986, and Landman (2016). Data for the Rincon Range is from Landman, 2016. Ages of volcanism in the Ocate and Raton-Clayton Fields are from Olmstead and McIntosh, 2004, and Nereson et al., 2013." The yellow box outline represents the area shown in Figure 31 of the Southern Sangre de Cristo Mountains.

The final dataset from Landman (2016) builds out from the Southern Sangre de Cristo region by acquiring low-temperature dates along the I-40 highway running E-W from Albuquerque, New Mexico, to Amarillo, Texas. AFT and AHe done on Triassic redbeds record reset dates from subsequent exhumation rather than detrital apatite dates.

Both AFT and AHe get progressively older to the east. Miocene AHe dates range from 25-10 Ma, closely resembling those seen in the Rincon Range Front (Figure 31). These are also similar to the AHe dates observed at the Spanish Peaks in Colorado. However, AFT dates are much older, which could be due to slower exhumation, or an earlier event being recorded. The four samples to the east, into the Texas Panhandle, are all Oligocene. One outlier at 53∓21 Ma stands out as being much older. The distance between samples leads to ambiguity as to the timing of exhumation further into the Great Plains.

Dates to the very west of Figure 32, from the Hagan and Sandia Mountains, record younger Miocene dates (House et al., 2003). However, these are likely a result of Rio Grande Rifting to the west and therefore are not considered to be a signal of the Miocene exhumation event focused on in this study.

Conclusions made in Landman (2016) suggest this trend is caused by hydration of the lithosphere following the Farallon slab breakoff that would have taken place during the Oligocene. Breakoff would have promoted elevated heat flow, leading to increased geothermal gradients, potentially locking in Oligocene AFT and AHe dates related to changing heat profiles rather than exhumation of any kind.

5.2.5. The Western Extent of the Ogallala Formation

The aforementioned Ogallala Formation is a highly important aquifer for much of the Eastern United States. Sourced from riverine deposition from Rocky Mountains erosion, estimates used in this study put the start of its deposition at 12-9.5 Ma (Smith et al., 2016; Zakrzewski, 1988; Tedford et al., 2004). The question still remains as to how far west the formation once extended and when deposition ceased.

New data from this study presents evidence of exhumation continuing from ~18-8 Ma in south-central Colorado (Spanish Peaks region). At 8 Ma, Huerfano Butte, located in the sedimentary basin at the western edge of the Great Plains, was actively eroding. This would indicate during the Ogallala's deposition, it never would have reached the Spanish-Peaks region.
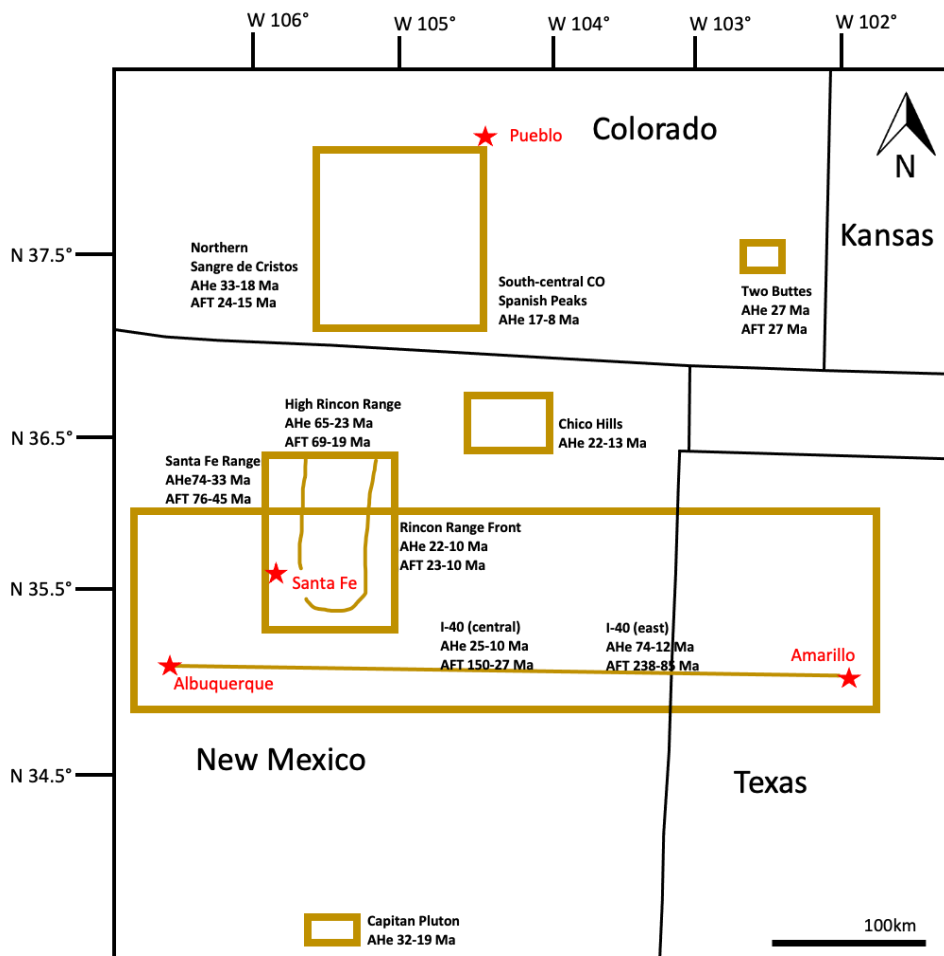
5.2.6. Regional Trends and Patterns

Figure 33: Summary map of low-temperature thermochronology dates from this study and Landman (2016).

Taking all our described data into account, the large-scale patterns and timing of exhumation begin to fall into place.

First looking in the north-south direction, youngest AHe dates are seen at Huerfano Butte in South-central Colorado (8 Ma), then get slightly older to the south at the Rincon Range Front and I-40 (central) samples. As aforementioned, Capitan Pluton records older exhumation in the Oligocene-early Miocene, which led Landman (2016) to suggest a south-to-north erosional pattern.

To the west of the Spanish Peaks, dates in the Colorado Sangre de Cristo Mountains get slightly older (Rickets et al., 2015; Lindsey et al., 1986), with Oligocene to early Miocene AHe and AFT. When looking at a similar distance in the Southern Sangre de Cristos of New Mexico, dates get significantly older, less than 25 km to the west (Figure 33), recording Late Cretaceous exhumation.

Similarly to the east, dates again get older, but over a much larger lateral distance (200km). In southeast Colorado, the Great Plains show Oligocene exhumation at 27 Ma from Two Buttes. In the plains of northeast New Mexico, the Chico Hills have slightly older Miocene dates (22-18Ma). Samples along the I-40 corridor of eastern-central New Mexico progressively get older as we look east into the Texas Panhandle, at around Late Eocene to Oligocene in age. Whereas those just south of the Chico Hills in the I-40 (central) are similarly Oligocene-Miocene.

If all these areas are recording the same event, this would suggest that exhumation stopped at the edges of the study region first in the Great Plains, Capitan Pluton, and the Southern Sangre de Cristos. Meanwhile, places like the Rincon Range Front and the Spanish peaks continued eroding until the mid-late Miocene. The Rincon Range Front is at the center of our region of interest, which could serve as an indicator that this may have been the focus of exhumation, with the greatest magnitude of erosion taking place. However, even later AHe at Huerfano Butte suggests that the northern extent continued even after the event had stopped in central-New Mexico.

5.2.7. Potential Causes of Oligo-Miocene Exhumation

A range of potential causes could lead to km-scale exhumation such as that observed in southeast Colorado and eastern New Mexico. These include (1) climate change, (2) tectonic uplift, and/or (3) drainage reorganization (Abbott et al., 2022; Molnar & England, 1990). Each of these will be explored to evaluate how strong each mechanism could explain exhumation patterns.
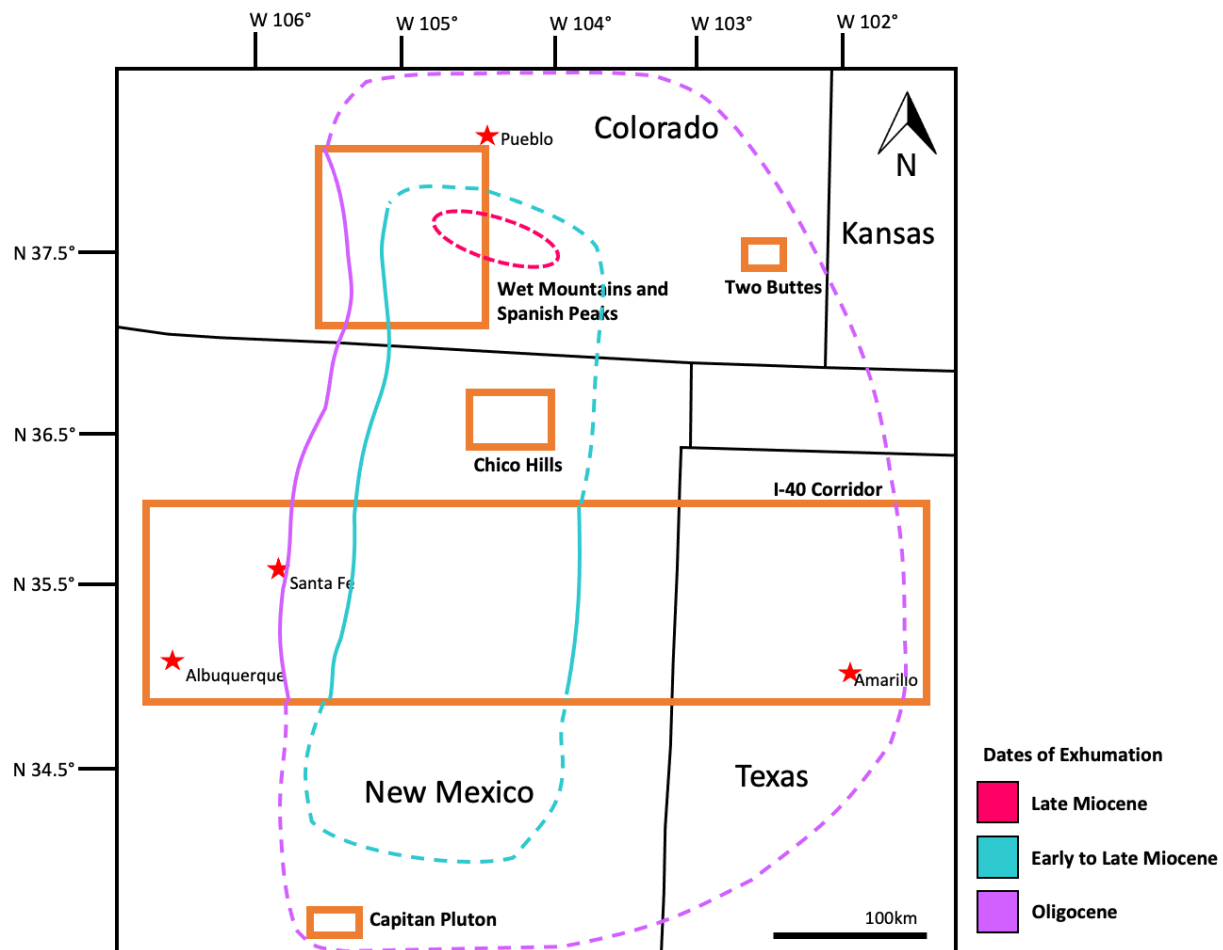
Figure 34: Rough estimated contours of Oligo-Miocene exhumation in areas of Southeast Colorado, East New Mexico, and the eastern Panhandle of Texas. Orange boxes represent regions with low-temperature thermochronology dates to constrain these contours. Dashed lines indicate greater uncertainty of contour boundaries.

Climate change

Landman (2016) suggests the Miocene signal recorded in the Rincon Range Front of the Southern Sangre de Cristo Mountains is a result of climate change. The onset of the Mid-Miocene Climate Optimum at 15 Ma (Zachos et al., 2001) could explain many of the AHe dates seen in this area. However, some dates are slightly older than 15 Ma which predates expected erosion brought about by this climate optimum. It is possible that these values are outliers and may be a result of less accurate dates. Upon looking at the data tables (Landman, 2016), outlier samples only have ~2 apatite aliquots as opposed to 5, meaning they could be inaccurate representations of exhumation timing.

On the other hand, if these are accurate dates, this would give evidence against the climate change hypothesis. No other sample sets yielded dates as young as 15 Ma, apart from some in the Spanish Peaks. However, the older dates from south-central Colorado put exhumation starting at 17 Ma. If climate change-induced exhumation was a large driving force, one would expect more of these Miocene dates to be recorded elsewhere. New data from Two Buttes puts erosion of the Colorado Great Plains at 27 Ma, far too early to be explained by this climate optimum.

Further evidence that goes against climate change as the exhumation mechanism can be seen in the sedimentary units of the Great Plains, namely the White River Group. Formed from volcaniclastic sediments, the group was deposited in the late Eocene-early Oligocene throughout Colorado, Wyoming,

Nebraska, Montana, and North and South Dakota (Terry et al., 1998). In Colorado, the White River Group only extends as far south as the Palmer Divide, between Denver and Colorado Springs. The presence of this group to the north suggests minimal post-Eocene erosion, which greatly contrasts the km-scale exhumation documented to the touch of the Palmer Divide. Localized erosion of the group would not be expected if global climate change were the primary mechanism. While it is possible that it was never deposited in southern Colorado and New Mexico, the mountains just west have Ignimbrite Flare-up extrusive rocks (e.g. the Greenhorn Mountain lava flow), which would have been the ideal source of White River sediments. Moreover, detrital zircons found in southwest Kansas are dated to the Ignimbrite Flare-up (Smith et al., 2016), which would likely have come from the mountains. So, the fact that these appear to be missing in between Kansas and the Rocky Mountains would support that these sedimentary units once were present in the Great Plains of Colorado and New Mexico.

A final line of evidence against climate change is that if it were a viable mechanism, one would expect to find the youngest dates at highest elevations. Instead, the Sangre de Cristos of both Colorado and New Mexico have dates younger than those found in the Great Plains (Lindsey et al., 1986; Ricketts et al., 2015; Landman, 2016), the inverse of what is expected.

Tectonic uplift

Patterns of exhumation advocate for a smaller scale event than would be brought about by climate change. Another mechanism for this exhumation could be from tectonic forcings. Crustal shortening is ruled out, as the last big occurrence of this was during the Late Cretaceous Laramide Orogeny. Crustal extension starting at 28 Ma from the Rio Grande Rift could explain the majority of AHe dates, but struggles to explain why timing of erosion is older the further away from the proposed central region is. Furthermore, this is still an ongoing extension, centered further west than our region of interest, so is unlikely to be the driver of exhumation in the Great Plains.

The third option of tectonic forcing is an epeirogeny, in which uplift is less linear than aforementioned processes. So far, this seems like the most viable way to explain more concentric patterns observed (Figure 34). Additional evidence that supports a local epeirogeny taking place are the sedimentary units of the Great Plains. Just by looking at the depositional ages of sediments underlying the Ogallala, there is reason to believe more erosion was taking place to the south. Along the Front Range of northern Colorado, the White River Group of Eocene age underlies the Ogallala. In southern Colorado, where the northernmost samples from this study are, Cretaceous sediments from the Western Interior Seaway are present. Finally, in New Mexico, even older Triassic sediments are observed under the Ogallala. This would suggest greater magnitudes of erosion were taking place where youngest thermochronology dates were found.

While the mechanisms behind epeirogenic events are less understood, several theories have been proposed to understand elevations seen in the Rocky Mountains. These include: (1) lithospheric thinning, (2) isostatic rebound from Farallon slab detachment, or (3) mantle drips.

Landman (2016) proposes the Oligocene-Miocene exhumation seen along the I-40 corridor is from elevated lithosphere heating during Ignimbrite Flare-up volcanism. Humphreys et al. (2003) links this to hydration of the lithosphere during flat-slab subduction of the Farallon plate. Once detached, bowing up of the lithosphere and volcanism began, leading to post-Laramide uplift.

The mantle drip hypothesis, first proposed by Houseman & Molnar (1997), suggests that portions of the lithosphere can detach into the asthenosphere as a result of crustal thickening. In southeast

Colorado and eastern New Mexico, the thickening event would have been the Laramide Orogeny. Loss of mass from the bottom of the lithosphere could cause isostatic compensation to occur, raising the crust in an epeirogeny and triggering erosion. This would also cause the center of a proposed 'drip' to gain the most elevation, and subsequently be subject to erosion for a longer period of time. This would fit our data, with central areas, such as the Rincon Range Front, showing youngest AHe dates that get progressively older to the east (Two Buttes, Chico Hills, I-40 (east)), south (Capitan Pluton), and west (Sangre de Cristos). The only dataset that does not fit this trend is the Spanish Peaks to the very north, in which lower elevation samples are as young as 8 Ma.

Other regions throughout the Colorado Rocky Mountains have shown similar concentric patterns of erosion that contribute to the idea of serial mantle drips (Abbott et al., 2022; Garcia, 2011). The idea here is that a drip in one region will trigger another to be formed nearby. The oldest proposed location of this is of Eocene age, in central Colorado (Abbott et al., 2022). Here, AFT and AHe show a $>2.0 \times 10^4$ km^2 area between the Arkansas Hill and High Park in which youngest dates are found at the center of the study region, mirroring what is seen in southeast Colorado and eastern New Mexico. A second example is seen in the West Elk Mountains, further west, in which a $\sim 1 \times 10^4$ km^2 sized area instead exhibits Miocene-early Pliocene low-temperature thermochronologic dates (Garcia, 2011; Abbott et al., 2021). Dubbed the 'Gothic Dome', this exhumation took place after both our exhumation and that in central Colorado (Figure 35).

The mantle drip hypothesis would allow for a mechanism that would lead to concentric exhumation in southeast Colorado and eastern New Mexico. However, some inconsistencies surrounding this theory include the difference in scale in this region. While the Gothic Dome and central Colorado centers are both roughly 100 km in diameter, our exhumation is ~500km in the N-S direction and ~300km E-W. While this may disagree with mantle drip theories, it is not enough evidence to completely dismiss it. The concept of drips is relatively new and ideas surrounding size and location are not yet set in stone.
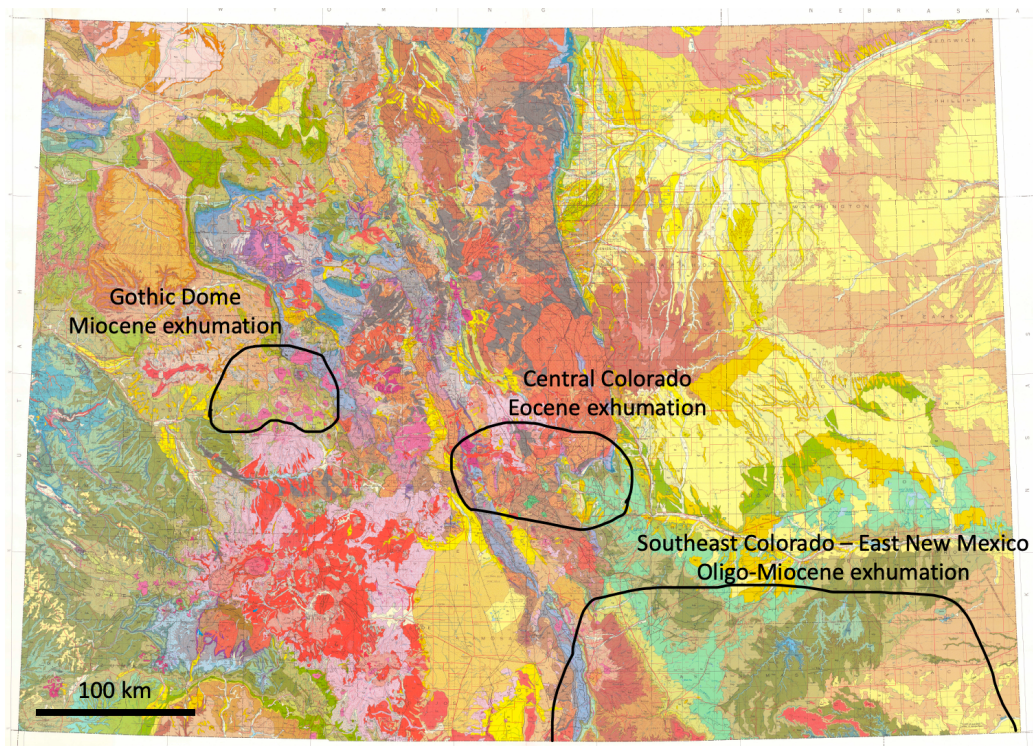

Figure 35: Approximate locations of concentric patterns of erosion in Colorado.

Drainage reorganization

The final mechanism for exhumation is drainage reorganization. This is dismissed as a possible reason for overall patterns seen, as there is little evidence of large-scale changes in drainage patterns between the Laramide Orogeny and Oligocene (Abbott et al., 2022; Scott, 1975; Epis et al., 1976), and thus is unable to explain older dates in our area of interest.

While it may not be a viable mechanism for large-scale erosion, the potential of later drainage reorganization, unrelated to any epeirogeny, could help explain the young dates in the Raton Basin.
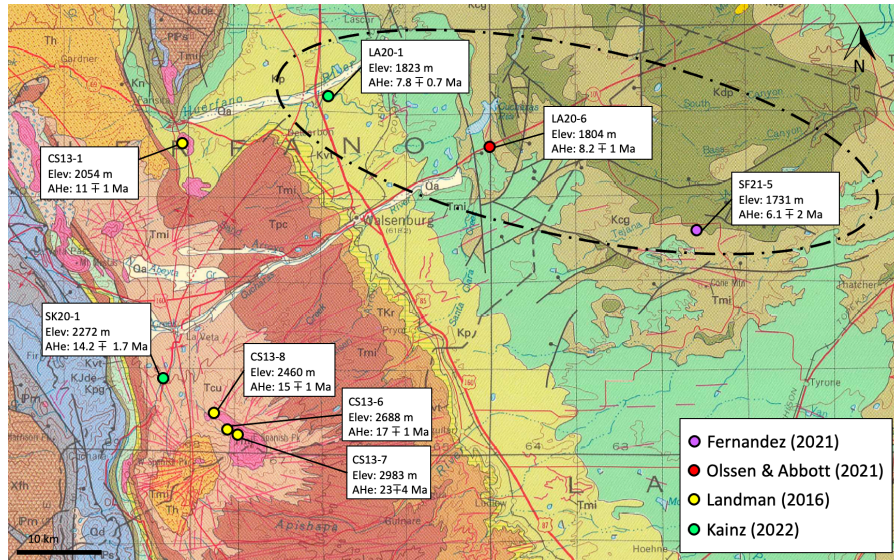

Figure 36: AHe dates from the South-central Rocky Mountains and igneous intrusions in the Great Plains (Fernandez, 2021; Olssen & Abbott, 2021). Dashed oval highlights dates younger than 8 Ma.

As discussed above, the one region that does not fit with the pattern of younger dates on the rim of our proposed exhumation area is in South-central Colorado. Two additional dikes in the Great Plains extend erosion to 6 Ma (Fernandez, 2021; Olssen & Abbott, 2021). It is possible that Miocene exhumation was overwritten by drainage reorganization of the Arkansas River 5-10 m.y.a, and this was fairly localized such that the signal was only picked up in the Raton Basin. The Arkansas River is thought to have been rerouted from the Rio Grande Rift into the plains of southeast Colorado in the last 10-20 Ma.

The main point that argues against this is how well Huerfano Butte fits in with the inferred rate of erosion of the Spanish Peaks (Figure 20). However, it is important to note that Figure 20 is not a vertical transect and thus must not be given too much weighting in terms of erosion timing compared with the Spanish Peaks due to spatial distance.

Alternative events recorded by low-temperature thermochronology

There is the possibility that AHe and AFT dates recorded are not products of erosion at all, but rather from large changes in geothermal gradients. Landman (2016) attributes Eocene-Oligocene dates in eastern New Mexico to be from elevated heat flow in the lithosphere due to break off of the Farallon slab (Rickett et al., 2015). In this case, dates would be a record of when the lithosphere began to cool, having nothing to do with exhumation. We do not deny the occurrence of this phenomenon, but whether it could provide low-temperature thermochronology dates documented is another matter. AHe from the Chico Hills complex and Rincon Range Front tell of a later exhumation event. It is possible that multiple working mechanisms could give patterns seen in this study. However, data is consistent with one

dominant event that was recorded in thermochronometers throughout the study region, best explained by an epeirogeny.

5.3. Errors and Uncertainties

A range of factors must be taken into consideration that may decrease reliability of data and inferences made. All stages of this study have aimed to reduce any uncertainty through precise practices and careful interpretation. However, it is still important to give thought to these potential areas of error.

5.3.1. Field Sampling and Apatite Selection

There is always risk of collecting samples that may have undergone more localized alterations, and are therefore not representative of regional-scale exhumation. An important factor to consider is reheating of an igneous body via nearby volcanism or fluids. While other thermochronologic studies may wish to investigate multiple stages of burial and exhumation, our region is relatively young, so dates are assumed to be straightforward cooling from emplacement. The main location where this may be an issue is in the Chico Hills, where heating from the Jemez Lineament may have caused resetting of AHe dates. However, samples were chosen far from Jemez volcanics, and dates were all too old to be explained by Jemez heating (10Ma), leading us to confidently reject this hypothesis.

The other main source of receiving inaccurate dates is from poor picking of apatite grains. Issues with fluid or mineral inclusions can alter helium diffusion kinetics, leading to dates that do not represent exhumation. Some samples, such as SK21-3, had apatite grains with a lot of surface relief which can hide inclusions. While a lot of effort was put into avoiding these types of grains, hidden inclusions can be difficult to identify. General consistency in individual grain dates within samples argues against this being an issue.

5.3.2. Interpretation Uncertainty

One of the biggest roadblocks to successful interpretation is the geothermal gradient. Those used in this study, from Berkman & Watterson (2010), are modern estimates. Inferences of the heat profiles in the Oligo-Miocene are hard to determine. Moreover, geothermal gradients are subject to change over short depths and lateral distances.

---

6. Conclusion

6.1. Main Findings

This study has presented new apatite (U-Th)/He data from the Great Plains of Colorado and New Mexico, consistent with previously found low-temperature thermochronologic data. Trends seen from Landman (2016) show young Miocene AHe and AFT in eastern-central New Mexico that get gradually older to the east, and rapidly older to the west. Very similar patterns exist in southeast Colorado, with the

Spanish Peaks and Raton Basin presenting mid-late Miocene AHe. Here, recorded exhumation gets older to the west in the Sangre de Cristos (Rickett et al., 2015; Lindsey et al., 1986), and older to the east at Two Buttes, both of which record Oligocene dates. The southernmost samples from Landman (2016) show Oligocene dates at Capitan Pluton, suggesting exhumation ended earlier in the south than it did in the north. In all areas, AHe and AFT indicate kilometer-scale erosion took place in the Great Plains during the Cenozoic.

The dynamic tectonic and climatic conditions of the Cenozoic in the American West make it difficult to conclude whether a single event caused exhumation patterns observed in this study, or if multiple mechanisms could be at play. A variety of causes have been identified, including Miocene global warming, effects from the Rio Grande Rift, heating from the Jemez Lineament, and elevated geothermal gradients in the Oligocene. A more simplistic approach to interpreting these would be that a single event dominated exhumation at this time. The simplest hypothesis is that the region was affected by an epeirogeny, causing a focus of elevation gain in northeast New Mexico. This would create an area of rapid erosion that could potentially get less intense the further away you look. Only the samples from southeast Colorado are inconsistent with this reasoning. However, a later event in this locality may have overwritten earlier exhumation, such as drainage reorganization.

6.2. Future Research

Research from this study has shown the benefit of targeting igneous rocks emplaced within sedimentary units to record the most accurate timing of exhumation events. This gives great insight into elevation gained within the Great Plains, as not much low-temperature thermochronology has been done to the east of the Rocky Mountains thus far. While sampling at the Two Buttes lamprophyre provided new information on Great Plains erosion, this remains as a single reference point, nearly 200km away from any other AHe/AFT data. Dikes and other intrusions, such as Huerfano Butte and Mica Butte (Fernandez, 2021), exist throughout the Great Plains and would make appropriate targets to sample in future studies. These would better constrain the northern and eastern edges of Oligo-Miocene exhumation.

Comparisons to northern Colorado would provide larger-scale regional trends, and exhumation of the Front Range region has not yet been explored. While many studies have completed low-temperature thermochronology in the Colorado Rocky Mountains, the majority of these are on crystalline basement rocks that dominate the area. Our region of study is unique in that volcanism from the Ignimbrite Flare-up and Rio Grande rifting emplaced an abundance of igneous intrusions into the Great Plains. These are not as common in the north, but some suitable targets in the plains of northeast Colorado present logical next steps in this research. Examples of these include the Valmont Dike and Flagstaff Sill, both within Boulder County n(via personal communication with Lon Abbott, 2022).

7. Acknowledgements

I would like to say thank you to Lon Abbott, for spending countless hours working on this project with me. I truly could not have asked for a better advisor. Thank you for teaching me how to read the rocks and tell fascinating stories from them. You have shown me that it's okay if science doesn't go the way you planned, and that it can lead to so many more, exciting discoveries.

Thank you, Becky Flowers, for seeing the potential in me since freshman year and for being an amazing role model. I've learned more from being in your lab group than I have in any class. Thanks to Jim Metcalf for showing me the ins and outs of (U-Th)/He and all the insight on how to read data. To Jeff Benowitz, for keeping me company while picking grains with some great conversation, and for getting my little apatites off to be destroyed so quickly. Thank you to Peter Martin for taking the time to walk me through his code to make my HeFTy plots look so great, and for helping me realize the importance of why good figures matter.

Thank you to Katherine Lininger, for being on my committee and for leading one of the best classes I have ever taken.

Thank you to Semele Yuan for showing me what it means to be a geologist. Your passion may have been the most influential factor growing up. I'm so grateful that I love what I do everyday, and that is all thanks to you.

Finally, thank you, Dad, for showing me the beauty of being outside. While other people may not care what rock I've got to show off, your careful ear means the world to me. Mum, for giving me the drive to be the best I can be, and for being the strong person I look up to. To Mary Grace, for teaching me how to be a kind person. And, to Nat, I suppose. I love you and miss you all so much.

8. Bibliography

Abbott, L. and Cook, T., 2012. *Geology Underfoot Along Colorado's Front Range*. Mountain Press Publishing Company.

Abbott, L., Flowers, R., Metcalf, J.,, Hiett, C., Kelleher, R., Camm, H., Ramba, M., McCorkel, N., Riccio, E., 2021; The Gothic Dome: Kilometer-scale Miocene Exhumation in Colorado's Elk and West Elk Mountains; Earth and Space Science Open Archive; p4; 2021; https://doi.org/10.1002/essoar.10508533.1

Abbott, L.D., Flowers, R.M., Metcalf, J., Falkowski, S., and Niazy, F., 2022, Post-Laramide, Eocene epeirogeny in central Colorado—The result of a mantle drip?: Geosphere, v. 18, no. X, p. 1–24, https://doi.org/10.1130/GES02434.1.

Ayotte, J., Flanagan, S., Morrow, W., 2007, Occurrence of Uranium and 222 Radon in Glacial and Bedrock Aquifers in the Northern United States, 1993-2003 Scientific Investigations Report 2007-5037

Berkman, F.E., and Watterson, N.A., 2010, Interpretive Geothermal Gradient Map of Colorado: Colorado Geological Survey map MS-51, scale 1:500,000.

Cather, S.M., Chapin, C.E., and Kelley, S.A., 2012, Diachronous episodes of Cenozoic erosion in southwestern North America and their relationship to surface uplift, paleoclimate, paleodrainage, and paleoaltimetry: Geosphere, v. 8, no. 6, p. 1177–1206, https:// doi .org /10 .1130 /GES00801 .1.

Chapin, C.E. and Kelley, S.A., 1997. The Rocky Mountain erosion surface in the front range of Colorado. Rocky Mountain Association of Geologists, 1997

Cherniak, D.J., 2019; Diffusion of helium in radiation-damaged zircon, Chemical Geology, Volume 529, 2019, 119308, ISSN 0009-2541, https://doi.org/10.1016/j.chemgeo.2019.119308.

Cross, T., Pilger, R., 1978; Tectonic controls of late Cretaceous sedimentation, western interior, USA. *Nature* **274,** 653–657 (1978). https://doi.org/10.1038/274653a0

Davis, L.L., Smith, D., McDowell, F.W., Walker, N.W., Borg, L.E., 1996; Eocene potassic magmatism at Two Buttes, Colorado, with implications for Cenozoic tectonics and magma generation in the western United States. *GSA Bulletin* 1996;; 108 (12): 1567–1579. doi: https://doi.org/10.1130/0016-7606(1996)108<1567:EPMATB>2.3.CO;2

Eaton, G.P., 2008; Epeirogeny in the Southern Rocky Mountains region: Evidence and origin. *Geosphere* 2008;; 4 (5): 764–784. doi: https://doi.org/10.1130/GES00149.1

Epis, R.C., Scott, G.R., and Chapin, C.E., 1976, Cenozoic volcanic, tectonic, and geomorphic features of central Colorado: Colorado School of Mines Professional Contribution, v. 8, p. 323–338.

English, J.M., Johnston, S.T., 2004; The Laramide orogeny: What were the driving forces?. International Geology Review. 2004 Sep 1;46(9):833-8. https://doi.org/10.2747/0020-6814.46.9.833

Farley, K.A., 2000, Helium diffusion from apatite: General behavior as illustrated by Durango fluorapatite: Journal of Geophysical Research, v. 105, p. 2903–2914, https:// doi .org /10 .1029 /1999JB900348.

Fernandez, S., S. Kainz, A. Olsson, L.D. Abbott, J.R. Metcalf, and R.M. Flowers, 2021, A (U-Th)/He Thermochronologic Investigation of Exhumation on the Great Plains of Southeastern Colorado and Northeastern New Mexico, AGU Fall Meeting, New Orleans, LA.

Flowers, R.M., Ehlers, T.A., 2018; Rock erodibility and the interpretation of low-temperature thermochronologic data, Earth and Planetary Science Letters, Volume 482, 2018, Pages 312-323, ISSN 0012-821X, https://doi.org/10.1016/j.epsl.2017.11.018.

Flowers, R.M., Ketcham, R.A., Shuster, D.L., Farley, K.A., 2009, Apatite (U–Th)/He thermochronometry using a radiation damage accumulation and annealing model, Geochimica et Cosmochimica Acta, Volume 73, Issue 8, 2009, Pages 2347-2365, ISSN 0016-7037, https://doi.org/10.1016/j.gca.2009.01.015.

Frye, J.C., Leonard, A.B. and Glass, H.D., 1982. *Western extent of Ogallala Formation in New Mexico* (Vol. 175). New Mexico Bureau of Mines & Mineral Resources.

Garcia, R.V., 2011, Cenozoic intrusive and exhumation history of the Elk and West Elk mountain plutons, Southwest Colorado [M.S. thesis]: Socorro, New Mexico Institute of Mining and Technology, 143 p.

Hansen, S.M., Dueker, K.G., Stachnik, J.C., Aster, R.C., and Karlstrom, K.E., 2013, A rootless rockies—Support and lithospheric structure of the Colorado Rocky Mountains inferred from CREST and TA seismic data: Geochemistry, Geophysics, Geosystems, v. 14, p. 2670–2695, https:// doi .org /10 .1002 /ggge .20143.

House, M.A., Kelley, S.A., and Roy, M., 2003, Refining the footwall cooling history of a rift flank uplift, Rio Grande rift, New Mexico: Tectonics, v. 22, no. 5, p. n/a–n/a, doi: 10.1029/2002TC001418.

Houseman, G.A., Molnar, P., 1997; Gravitational (Rayleigh–Taylor) instability of a layer with non-linear viscosity and convective thinning of continental lithosphere, *Geophysical Journal International*, Volume 128, Issue 1, January 1997, Pages 125–150, https:// doi .org /10 .1111 /j .1365 -246X .1997 .tb04075 .x.

Humphreys, E., Hessler, E., Dueker, K., Farmer, L., Erslev, E., Atwater, T., 2003; How Laramide-Age Hydration of North American Lithosphere by the Farallon Slab Controlled Subsequent Activity in the Western United States, International Geology Review, 45:7, 575-595, doi: 10.2747/0020-6814.45.7.575

Jones, C.H., Farmer, G.L., Sageman, B., and Zhong, S., 2011, Hydrodynamic mechanism for the Laramide orogeny: Geosphere, v. 7, no. 1, p. 183–201, https:// doi .org /10 .1130 /GES00575 .1.

Kainz, S., Abbott, L., Flowers, R., and Metcalf, J., 2021, Effect of rock strength on the documentation of an exhumation event using low temperature thermochronology: The south-central Colorado example: European Geological Union abstracts. EGU General Assembly 2021: Online (Bergheim), v. 4–8, p. EGU2021–EGU13071, https:// doi .org /10 .5194 /egusphere -egu21 -13071.

Kelley, S.A., and Chapin, C.E., 2004, Denudation history and internal structure of the Front Range and Wet Mountains, Colorado, based on apatite-fission-track thermochronology, *in* Cather, S.M., et al., eds., Tectonics, Geochronology, and Volcanism in the southern Rocky Mountains and Rio Grande Rift: New Mexico Bureau of Geology and Mineral Resources Bulletin, v. 160, p. 41–68.

Kelley, S.A., Chapin, C.E., Bauer, P.W., 1995. Apatite fission-track thermochronology of southern Rocky Mountain–Rio Grande rift–western High Plains provinces. In *Geology of the Santa Fe region: New Mexico Geological Society Field Conference Guidebook* (Vol. 46, pp. 87-96).

Kelley, S.A., Chapin, C.E., and Corrigan, J., 1992, Late Mesozoic to Cenozoic cooling histories of the flanks of the northern and central Rio Grande Rift, Colorado and New Mexico: New Mexico Bureau of Geology & Mineral Resources Bulletin, v. 145.

Kelley, S.A., Duncan, I.J., 1986. Late Cretaceous to middle Tertiary tectonic history of the northern Rio Grande rift, New Mexico. *Journal of Geophysical Research: Solid Earth*, *91*(B6), pp.6246-6262. https://doi.org/10.1029/JB091iB06p06246

Ketcham, R.A., 2005, Forward and inverse modeling of low-temperature thermochronometry data, in Reiners, P.W., and Ehlers, T.A., eds., Low-temperature thermochronology: techniques, interpretations, and applications: Reviews in Mineralogy and Geochemistry 58, p. 275–314. doi: https://doi.org/10.2138/rmg.2005.58.11

Kron, A, and Heiken, G. 1980. Geothermal gradient map of the United States. https://www.osti.gov/servlets/purl/5354021.

Landman, R.L., 2016, Thermochronologic investigations of Cenozoic unroofing and surface uplift in the southern Rocky Mountains and Great Plains [Ph.D. thesis]: Boulder, University of Colorado.

Leonard, E.M., 2002. Geomorphic and tectonic forcing of late Cenozoic warping of the Colorado piedmont. *Geology*, *30*(7), pp.595-598. https://doi.org/10.1130/0091-7613(2002)030<0595:GATFOL>2.0.CO;2

Lindsey, D.A., Andriessen, P.A.M., Wardlaw, B.R., 1986; Heating, cooling, and uplift during Tertiary time, northern Sangre de Cristo Range, Colorado. *GSA Bulletin* 1986;; 97 (9): 1133–1143. doi: https://doi.org/10.1130/0016-7606(1986)97<1133:HCAUDT>2.0.CO;2

Litton, S., 2020; A Petrologic Study of Huerfano Butte Lamprophyre.

Lord, A.B.H., McGregor, H., Roden, M.F., Salters, V.J.M., Sarafian, A., and Leahy, R., 2016, Petrogenesis of coeval sodic and potassic alkaline magmas at Spanish Peaks, Colorado: Magmatism related to the opening of the Rio Grande rift: Geochimica et Cosmochimica Acta, v. 185, p. 453–476, https:// doi .org /10 .1016 /j .gca .2016 .04 .019.

Martin, P.E., 2021; HeFTy GOF Plotter; https://github.com/Peter-E-Martin/HeFTy_GOFplotter

McIntosh, W. C., Chapin, C. E., & Cather, S. M. (2004). Geochronology of the central Colorado volcanic field. *New Mexico Bureau of Geology and Mineral Resources Bulletin*, *160*, 205-238.

Metcalf, J.R., Flower, R.M., 2021; (U-Th)/He Chronology. Applied Geology, Geochronology: 66-75.

Molnar, P., and England, P., 1990, Late Cenozoic uplift of mountain ranges and global climate change: Chicken or egg?: Nature, v. 346, p. 29–34, https:// doi .org /10 .1038 /346029a0.

Penn, B.S., Lindsey, D.A., 2009; ^{40}Ar/^{39}Ar dates for the Spanish Peaks intrusions in south-central Colorado. *Rocky Mountain Geology* 2009;; 44 (1): 17–32. doi: https://doi.org/10.2113/gsrocky.44.1.17

Pilione, L. J., Gold, D. P., and Kreiger, E.W., 1977, Fission track age of apatite from a lamprophyre dike in the Two Buttes igneous complex, southeastern CO: Geological Society of America Abstracts with Programs, v. 9, p. 641–642.

Reiners, P. W., Carlson, R. W., Renne, P. R., Cooper, K. M., Granger, D. E., McLean, N. M., & Schoene, B. (2017). *Geochronology and thermochronology*. John Wiley & Sons.

Ricketts, J.W., Kelley, S.A., Karlstrom, K.E., Schmandt, B., Donahue, M.S., and van Wijk, J., 2015, Synchronous opening of the Rio Grande rift along its entire length at 25–10 Ma supported by apatite (U-Th)/He and fission-track thermochronology, and evaluation of possible driving mechanisms: Geological Society of America Bulletin, v. 128, p. 397–424, https:// doi .org /10 .1130 /B31223 .1.

Scott, G R, Wilcox, R E, and Mehnert, H H., 1990; Geology of volcanic and subvolcanic rocks of the Raton-Springer area, Colfax and Union Counties, New Mexico, United States Geological Survey, Professional Paper; (USA), Journal Volume: 1507

Scott, G.R., 1975, Cenozoic surfaces and deposits in the Southern Rocky Mountains, *in* Curtis, B.F., ed., Cenozoic History of the Southern Rocky Mountains: Geological Society of America Memoir 144, p. 227–248, https:// doi .org /10 .1130 /MEM144 -p227.

Staatz, M.H., 1985, Geology and description of the thorium and rare-earth veins in the Laughlin Peak area, Colfax County, New Mexico: U.S. Geological Survey Professional Paper 1049-E, p. E1-E32.

Tedford, R.H., 2004; Miocene mammalian faunas, Ogallala Group, Pawnee Buttes area, Weld County, Colorado. *Bulletin of Carnegie Museum of Natural History* 2004.36 (2004): 277-290.

Terry, D.O., LaGarry, H.E. and Hunt, R.M. eds., 1998. *Depositional environments, lithostratigraphy, and biostratigraphy of the White River and Arikaree Groups (late Eocene to early Miocene, North America)* (Vol. 325). Geological Society of America.

Tweto, O., 1979, Geologic map of Colorado, U.S. Geological Survey, scale 1:500,000.

Vermeesch, P., Tian, Y., 2014, Thermal history modelling: HeFTy vs. QTQt, Earth-Science Reviews, Volume 139, 2014, Pages 279-290, ISSN 0012-8252, https://doi.org/10.1016/j.earscirev.2014.09.010.

Weisberg, W.R., Metcalf, J.R., Flowers, R.M., 2018; Distinguishing slow cooling versus multiphase cooling and heating in zircon and apatite (U-Th)/He datasets: The case of the McClure Mountain syenite standard, Chemical Geology, Volume 485, 2018, Pages 90-99, ISSN 0009-2541, https://doi.org/10.1016/j.chemgeo.2018.03.038.

Zachos, J., Pagani, M., Sloan, L., Thomas, E., and Billups, K., 2001, Trends, rhythms, and abberations in global climate 65 Ma to present: Science, v. 292, p. 686–693, https:// doi .org /10 .1126 /science .1059412.

Zakrzewski, R. J., and M. E. Nelson., 1988; Preliminary report on fossil mammals from the Ogallala (Miocene) of north-central Kansas. *Geology, paleontology, and Biostratigraphy of Western Kansas. Fort Hays Studies, third series, Science* 10 (1988): 117-127.

9. *Appendix*

Table 2: Detailed Reporting Table for Apatite (U-Th)/He Data

Sample Name and aliquot[a]	length 1 (µm)[b]	width 1 (µm)[c]	length 2 (µm)[b]	width 2 (µm)[d]	Geometry[e]	Np[f]	Mass (µg)[g]	^{4}He (ncc)[h]	±[i]	U (ng)[j]	±[i]	Th (ng)[k]	±i	^{147}Sm (ng)[l]	±[h]	F_T ^{238}U[m]	F_T ^{235}U[m]	F_T ^{232}Th[m]	F_T ^{147}Sm[m]
South-central Colorado																			
LA20-1: Huerfano Butte ultramafic lamprophyres, 37°45'13" N, 104°49'38" W, 1823m																			
LA20-1_a01	337.9	116.1	325.5	99.8	4	0	8.168	0.063	0.001	0.030	0.001	0.258	0.004	0.142	0.002	0.773	0.738	0.733	0.927
LA20-1_a02	308.8	115.3	308.7	79.1	4	0	5.219	0.065	0.001	0.022	0.001	0.168	0.003	0.116	0.002	0.719	0.676	0.670	0.909
LA20-1_a03	223.3	161.9	226.5	142.7	4	1	8.949	0.124	0.001	0.054	0.002	0.459	0.004	0.155	0.001	0.817	0.789	0.785	0.941
LA20-1_a04	203.7	122.5	203.9	91.6	4	0	4.493	0.025	0.001	0.013	0.000	0.082	0.002	0.088	0.002	0.742	0.703	0.697	0.916
LA20-1_a06	169.4	102.6	172.2	91.9	4	0	3.493	0.015	0.000	0.010	0.001	0.061	0.001	0.071	0.001	0.733	0.693	0.687	0.914
SK20-1: Porphyritic intemediate dike from the Spanish Peaks, 37°27'31" N, 105°01'55" W, 2272m																			
SK20-1_a01	195.6	92.4	199.9	67.8	4	2	1.887	0.115	0.001	0.044	0.001	0.206	0.002	0.055	0.001	0.674	0.625	0.617	0.895
SK20-1_a02	322.2	112.7	321.6	81.6	4	2	4.793	0.243	0.002	0.103	0.002	0.530	0.006	0.105	0.002	0.736	0.695	0.689	0.915
SK20-1_a03	269.6	155.4	269.2	110.9	4	1	7.716	0.420	0.003	0.158	0.003	0.740	0.009	0.120	0.001	0.790	0.758	0.753	0.933
SK20-1_a04	249.4	108.2	250.1	76.8	4	1	3.565	0.167	0.001	0.073	0.003	0.340	0.006	0.058	0.002	0.711	0.667	0.660	0.907
SK20-1_a05	112.2	142.5	126.5	100.8	4	0	3.247	0.145	0.002	0.049	0.001	0.237	0.003	0.046	0.001	0.733	0.693	0.687	0.913
Chico Hills, NM																			
SK21-1: mafic Eagle Rock Dike, 36°39'55" N, 104°29'42" W, 1822m																			
SK21-1_a01	138.6	97.1	127.6	64.3	4	0	1	0.043	0.001	0.011	0.001	0.074	0.002	0.044	0.001	0.64	0.59	0.58	0.88
SK21-1_a02	173.2	95.0	228.6	71.2	4	0	3	0.062	0.001	0.025	0.000	0.133	0.003	0.062	0.001	0.69	0.65	0.64	0.90
SK21-1_a03	105.1	100.4	88.7	74.9	4	0	1	0.081	0.001	0.019	0.001	0.119	0.002	0.051	0.001	0.66	0.62	0.61	0.89
SK21-1_a04	100.0	94.2	84.1	54.0	4	0	1	0.083	0.001	0.019	0.001	0.130	0.003	0.046	0.001	0.58	0.53	0.52	0.86
SK21-1_a05	112.1	84.1	115.3	67.6	4	0	1	0.020	0.001	0.005	0.001	0.034	0.001	0.031	0.001	0.65	0.60	0.59	0.88
SK21-3: Piney Mtn Rd tephrite, 36°32'52" N, 104°09'20" W, 2300m																			
SK21-3_a01	228.8	122.7	227.1	109.4	4	1	6	0.623	0.005	0.038	0.001	1.439	0.025	0.118	0.002	0.78	0.75	0.74	0.93
SK21-3_a02	122.3	154.4	121.5	144.1	4	1	4	0.844	0.006	0.049	0.001	1.818	0.028	0.116	0.002	0.76	0.73	0.72	0.92
SK21-3_a03	191.4	84.6	177.7	66.8	4	0	2	0.910	0.005	0.120	0.003	2.212	0.039	0.140	0.002	0.67	0.62	0.62	0.89
SK21-3_a04	146.0	80.3	148.7	60.3	4	1	1	0.279	0.003	0.017	0.001	0.658	0.012	0.042	0.001	0.63	0.58	0.57	0.88
SK21-2: Slagle trachyte, 36°37'21" N, 104°15'58" W, 2054m																			
SK21-2_a01	112.9	180.2	70.3	133.0	4	0	4	0.299	0.002	0.059	0.001	0.593	0.010	0.146	0.002	0.76	0.73	0.72	0.92
SK21-2_a02	178.1	214.6	158.4	170.2	4	1	8	0.926	0.006	0.172	0.003	2.430	0.038	0.182	0.002	0.82	0.79	0.78	0.94
SK21-2_a03	334.1	106.0	313.6	75.8	4	1	5	0.004	0.000	0.070	0.003	0.706	0.012	0.138	0.002	0.72	0.68	0.67	0.91
SK21-2_a04	108.6	111.1	93.2	90.4	4	1	1	0.121	0.001	0.026	0.001	0.251	0.004	0.070	0.001	0.68	0.64	0.63	0.90
SK21-2_a05	335.2	168.5	307.5	118.6	4	1	11	0.711	0.003	0.184	0.004	1.422	0.042	0.205	0.002	0.81	0.78	0.77	0.94
Great Plains, SE Colorado																			
SK21-6: Two Buttes lamprophyres, 37°39'23" N, 102°32'17" W, 1326m																			
SK21-6_a01	152.9	109.3	132.4	89.1	4	1	2	0.705	0.005	0.200	0.005	0.522	0.005	0.060	0.001	0.72	0.68	0.67	0.91
SK21-6_a02	144.4	112.3	144.5	94.5	4	1	3	0.318	0.001	0.054	0.003	0.332	0.003	0.089	0.002	0.73	0.69	0.68	0.91
SK21-6_a03	128.7	97.3	114.8	79.1	4	1	2	0.318	0.003	0.061	0.001	0.262	0.002	0.077	0.002	0.68	0.64	0.63	0.89
SK21-6_a04	272.1	258.4	273.5	189.1	4	2	14	2.123	0.013	0.322	0.008	2.596	0.030	0.259	0.002	0.85	0.83	0.82	0.95

a - Sample and mineral being analyzed. a is apatite, z is zircon.

b - Length is measured parallel to the c-axis and includes pyramidal terminations. It is measured twice on two perpendicular sides.

c - Width 1 is measured perpendicular to the c-axis.

d - Width 2 is measured perpendicular to both the c-axis and width 1.

e - Geometry is defined as described as in Figure 3 of Ketcham et al., (2011). 1 is elliptical, 2 is cylindrical, 3 is orthogonal, and 4 is hexagonal. Each analyzed grain is a single whole crystal, not a fragment.

f - Np denotes the number of pyramidal terminations of the grain.

g - Mass is the mass of the crystal. Determined from the measured grain dimensions, the volume assuming the reported grain geometry, and the volume equations and mineral densities in Ketcham et al. (2011).

h - Blank-corrected 4He

i - Uncertainties on 4He, U, Th, and Sm are reported at 2s and include the propaged uncertainties on the measurements of the sample, blank, spike, and standard.

j - Total blank-corrected ng of 238U and 235U. Total 238U is measured and 235U is calculated assuming 235U = 238U/137.818

k - Total blank-corrected ng of 232Th

l - Total blank-corrected ng of 147Sm

m - Parent isotope-specific alpha ejection-corrections computing assuming the reported grain geometry, the equations and alpha-stopping distances in Ketcham et al., (2011), and homogeneous parent isotope distribution.